Rab GTPase- and class V myosin-dependent membrane tethering in a chemically defined system

Motoki Inoshita[1], Joji Mima[1]*

[1]Institute for Protein Research, Osaka University, Suita, Osaka, Japan

***For correspondence:**
Joji Mima
Institute for Protein Research, Osaka University, 3-2 Yamadaoka, Suita, Osaka 565-0871, Japan
Tel.: +81 6 6879 4326
Fax: +81 6 6879 4329
E-mail: Joji.Mima@protein.osaka-u.ac.jp

Running title:

Rab- and Myo5-mediated membrane tethering

Competing interests:
The authors have no competing interests to declare.

Funding:
The Ministry of Education, Culture, Sports, Science and Technology, Japan (MEXT) (to Joji Mima)

Abstract

Membrane tethering is a fundamental reaction to confer the specificity of membrane trafficking in eukaryotic cells. Although Rab-family GTPases and specific Rab-interacting effector proteins have been reported to be responsible for membrane tethering, whether and how these key components directly and specifically tether subcellular membranes still remain enigmatic. Using the chemically defined systems reconstituted with purified human Rabs and synthetic liposomes, we now establish that Rab-family GTPases have the conserved function to directly trigger membrane tethering, even in the absence of any types of Rab effectors. Furthermore, we strikingly demonstrate that membrane tethering mediated by endosomal Rab11a is selectively stimulated by the cognate Rab effectors, class V myosins, in a GTP-dependent manner. These findings postulate the novel concept that Rab proteins are a *bona fide* membrane tether to physically link two distinct lipid bilayers, and Rab effectors, including class V myosins, are rather a regulator of Rab-mediated membrane tethering.

Summary statement

Biochemical reconstitution studies reveal that human Rab GTPases are a *bona fide* membrane tether and class V myosin motors specifically promote membrane tethering mediated by their cognate Rab GTPase.

Introduction

All eukaryotic cells, from yeast to human cells, deliver the collect sets of the cargoes such as proteins and lipids to the appropriate cellular compartments including a variety of subcellular organelles, the plasma membrane, and the extracellular space (**Bonifacino and Glick, 2004**). These membrane trafficking events are a fundamental and highly selective process in the eukaryotic endomembrane systems, ensuring that transport vesicles or other membrane-bounded carriers specifically recognize, physically bind to, and eventually fuse with the target membranes in a spatiotemporally regulated manner (**Bonifacino and Glick, 2004**). A large body of prior genetic and biochemical studies have described miscellaneous key protein components functioning in eukaryotic membrane trafficking, which include SNAREs (soluble *N*-ethylmaleimide-sensitive factor attachment protein receptors) (**Jahn and Scheller, 2006**), SNARE-binding cofactors and chaperones such as Sec1/Munc18 proteins (**Baker and Hughson, 2016**), Rab-family small GTPases **(Stenmark, 2009**; **Hutagalung and Novick, 2011**), and Rab-interacting proteins termed "Rab effectors" (**Grosshans et al., 2006**; **Wandinger-Ness and Zerial, 2014**). Membrane tethering mediated by Rab GTPases and Rab effectors is generally known to be the first contact between the transport carriers and the target membranes and thus an essential step to determine the specificity of intracellular membrane trafficking (**Waters and Pfeffer, 1999**; **Cai et al., 2007**; **Yu and Hughson, 2010**), followed by SNARE-mediated membrane fusion, which is another critical layer to confer the fidelity of membrane trafficking (**Scales et al., 2000**; **McNew et al., 2000**; **Parlati et al., 2002**; **Izawa et al., 2012**; **Furukawa and Mima, 2014**). However, how Rab GTPases and Rab effectors work together to specifically drive membrane tethering has still remained elusive (**Brunet and Sacher, 2014**; **Tamura and Mima, 2014**), although recent biochemical reconstitution studies have begun to report the intrinsic membrane tethering potency of specific Rab effectors (**Yu and Hughson, 2010**; **Hickey and Wickner, 2010**; **Ho and Stroupe, 2015**; **Cheung et al., 2015**;

66 **Ho and Stroupe, 2016**; **Murray et al., 2016**) and Rab GTPases (**Lo et al., 2012**; **Tamura and Mima,**
67 **2014**). In this study, to gain a deeper insight into the mechanisms of intracellular membrane
68 tethering, we have reconstituted membrane tethering reactions in a chemically defined system
69 from synthetic liposomes and purified human Rab GTPases and class V myosins as the cognate
70 effectors of Rab11a, thereby comprehensively investigating their genuine functions in membrane
71 tethering.
72

Results and discussion

Prior two studies on membrane tethering in a chemically defined reconstitution system have described that tethering of synthetic liposomes can be directly triggered by several Rab-family GTPases themselves, which locate and function at the endosomal compartments in yeast (**Lo et al., 2012**) and human cells (**Tamura and Mima, 2014**). This Rab-mediated tethering of liposomal membranes is an efficient and specific biochemical reaction, as we established that membrane-anchored human Rab5a rapidly induced the formation of massive liposome clusters, and also that the tethering activity of Rab5a was able to be strictly and reversibly controlled by the membrane attachment and detachment of Rab proteins on both apposing membranes (**Tamura and Mima, 2014**). These our results strongly suggest the critical requirement of *trans*-Rab-Rab interactions on two distinct opposing membranes for a reversible membrane tethering event (**Tamura and Mima, 2014**).

In the current reconstitution study, to further comprehensively investigate the inherent membrane tethering potency of Rab-family GTPases in human, we purified and tested the six representative Rab GTPases functioning in the endocytic pathways (Rab4a, Rab5a, Rab7a, Rab9a, Rab11a, and Rab14) (**Wandinger-Ness and Zerial, 2014**), for typical non-endosomal Rabs, Rab1a in ER-to-Golgi traffic and Rab3a in exocytosis (**Stenmark, 2009**; **Hutagalung and Novick, 2011**), and also HRas for the control protein of a non-Rab small GTPase in the Ras superfamily (**Rojas et al., 2012**) (**Figure 1A**). All of the Rab-family and HRas GTPase proteins were purified as their full-length forms, consisting of the N-terminal non-conserved flexible segments (5-30 residues), the conserved globular Ras-superfamily GTPase domains in the middle (160-170 residues), and the so-called C-terminal hypervariable region (HVR) domains (20-50 residues) (**Rojas et al., 2012**) (**Figure 1A,B**; **Figure 1 – figure supplement 1**). In addition to the full-length amino acid sequences

of native proteins, to mimic membrane binding and anchoring of native Rab and HRas proteins through their isoprenyl or palmitoyl lipid anchors at the C-terminus (**Hutagalung and Novick, 2011**; **Rojas et al., 2012**), these recombinant Rab and HRas proteins used here were further artificially modified with a C-terminal polyhistidine tag (His12), which can be stably associated with synthetic liposomal membranes bearing a DOGS-NTA lipid (1,2-dioleoyl-sn-glycero-3-{[N-(5-amino-1-carboxypentyl)iminodiacetic acid]-succinyl}) (**Figure 1B**; **Figure 2A**). We employed GTPase activity assays for all of the purified Rab-His12 and HRas-His12 proteins, indicating that they retained the comparable intrinsic GTPase activities, which specifically converted GTP to GDP and a free phosphate (**Figure 1C**). Thus, this establishes that purified Rab-His12 and HRas-His12 proteins from the current preparations are all well folded and functionally active in solution (**Figure 1C**).

Dissecting the membrane tethering potency of human Rab GTPases in a chemically defined reconstitution system

The intrinsic potency of human Rab GTPases to directly drive membrane tethering was thoroughly evaluated by the kinetics of increase in turbidity of liposome suspensions in the presence of Rab proteins, which can be monitored by measuring the absorbance at 400 nm (**Figure 2**; **Figure 3**) (**Ohki et al., 1982**; **Hui et al., 2011**; **Tamura and Mima, 2014**; **Liu et al., 2015**). Rab-anchored liposomes were generated with purified Rab-His12 proteins and synthetic liposomes (400 nm in diameter) bearing a DOGS-NTA lipid and five major lipid species of phosphatidylcholine (PC), phosphatidylethanolamine (PE), phosphatidylinositol (PI), phosphatidylserine (PS), and cholesterol, roughly recapitulating lipid compositions of subcellular organelle membranes in mammalian cells (**Figure 2A**) (**van Meer et al., 2008**). With respect to Rab proteins tested in the tethering assays, as prior studies using the chemically defined reconstitution system had reported

121 the intrinsic tethering activity of several Rabs in the endocytic trafficking pathways of yeast (the
122 Rab5 ortholog Vps21p) (**Lo et al., 2012**) and human cells (Rab5a and Rab7a) (**Tamura and Mima,**
123 **2014**), first we selected six representative endosomal Rabs (Rab4a, Rab5a, Rab7a, Rab9a, Rab11a,
124 and Rab14) in human for comprehensively analyzing the tethering potency of Rab-family GTPases
125 (Figure 2B-G). By applying the liposome turbidity assay to the six Rab proteins at variable
126 concentrations, ranging from 0.5 μM to 4 μM towards 0.5 mM total lipids in the reactions (Figure
127 2A), rapid increase in liposome turbidity was triggered specifically either by Rab5a or Rab7a even
128 at the low protein concentrations (0.5–1.0 μM, corresponding to the protein-to-lipid molar ratios
129 of 1:1000–1:500) (Figure 2C,D). This establishes the very high potency of these two endosomal
130 Rabs to directly catalyze membrane tethering reactions *in vitro*, consistent with our prior study on
131 membrane tethering mediated by human Rabs (**Tamura and Mima, 2014**). Moreover, when
132 assayed with the high protein concentrations of Rabs such as 4 μM (protein-to-lipid ratio, 1:125),
133 we revealed that not only Rab5a and Rab7a (Figure 2C,D) but also all of the other endosomal Rabs
134 (Rab4a, Rab9a, Rab11a, and Rab14) retained the significant intrinsic capacity to initiate efficient
135 tethering of synthetic liposomes by themselves (Figure 2B,E,F,G). These data led us to propose
136 the conserved function for all the endosomal Rab-family GTPases to physically link two distinct
137 lipid bilayers together for membrane tethering events.
138
139 To what extent can the Rab protein densities on a membrane surface used in the current
140 liposome turbidity assays (Figure 2) recapitulate the physiological conditions at subcellular
141 membranes in mammalian cells? Using synaptic vesicles as a model of a trafficking organelle,
142 previous comprehensive proteomic and lipidomic analyses of highly purified synaptic vesicles
143 from rat brain determined the average copy numbers per vesicle of the major protein constituents
144 including Rab-family GTPases (**Takamori et al., 2006**). Those quantitative data indicate that, on

average, approximately 10 copies of Rab3a and 15 copies of the other Rab GTPases, thus 25 copies of Rab proteins in total are present in each single purified synaptic vesicle (**Takamori et al., 2006**). Assuming (i) this copy number of synaptic Rabs (25 copies/vesicle), (ii) a mean outer diameter of synaptic vesicles of 42 nm (**Takamori et al., 2006**), (iii) a typical bilayer thickness of 4 nm (**Nagle and Tristram-Nagle, 2000**), and (iv) an average area occupied by a single phospholipid molecule of 0.65 nm^2 (**Nagle and Tristram-Nagle, 2000**), we estimated the surface areas of the outer and inner lipid layers of synaptic vesicles (5,540 nm^2 and 3,630 nm^2, respectively) that bore 14,100 lipid molecules in total, thereby giving approximately the Rab protein-to-lipid molar ratio of 1:560 (25 Rabs/vesicle, 14,100 lipids/vesicle). It should be noted that, in the current chemically defined system, Rab5a and Rab7a (at least) can trigger rapid and efficient membrane tethering at the Rab-to-lipid molar ratio of 1:500 (Figure 2C,D, black bold lines), which is almost identical to the physiological ratio calculated above (Rab-to-lipid, 1:560). In addition to the Rab-to-lipid molar ratios, we also quantitatively estimated the membrane surface areas occupied by Rab proteins in the current reconstitution experiments (Figure 2). Assuming that (i) Rab proteins are typically a spherical 25 kDa protein with an average radius of 2.0 nm (**Erickson, 2009**), (ii) all of the Rab-His12 molecules added to the reactions are stably attached to liposomal membranes containing a DOGS-NTA lipid (Figure 2A), and (iii) a single 400-nm-diameter liposome contains 1,520,000 lipid molecules (the total surface area, 985,000 nm^2; the surface area/lipid, 0.65 nm^2) (**Nagle and Tristram-Nagle, 2000**), the percentages of the membrane surface coverage by Rab proteins were calculated to be in the range of 3.79% to 30.3% (0.5 μM – 4.0 μM Rab proteins; the Rab-to-lipid ratio, 1:1000 – 1:125) (Figure 2). These estimated values of the surface coverage by Rab proteins reflect that Rab proteins occupy only a minor portion of the membrane surface areas of liposomes in the turbidity assays and thus appear to have plenty of space to interact and cooperate with other proteins and lipids on the membranes. Taken together, the Rab-to-lipid molar ratios and

membrane surface areas occupied by Rabs that we estimated above support the idea that endosomal Rab proteins can drive rapid and efficient membrane tethering *in vitro* under the physiological or physiologically relevant conditions mimicking subcellular membranes in mammalian cells.

Our data of the current liposome turbidity assays have revealed the conserved membrane tethering potency of endosomal Rab proteins in the context of a physiologically relevant function (Figure 2B-G). Next, we asked whether the intrinsic membrane tethering potency of human Rabs is the specialized function exclusively for Rab-family small GTPase proteins among the Ras superfamily GTPases (**Rojas et al., 2012**) and, moreover, for the Rab proteins that are specifically localized at the endosomal compartments. To address this, we performed the turbidity assays for the HRas protein as the model of a non-Rab Ras-superfamily GTPase (Figure 3A,B) and for two of the well-studied non-endosomal Rab proteins, Rab1a in ER-to-Golgi traffic and Rab3a in exocytosis (Figure 3A,C,D), with the same range of the protein concentrations as tested in Figure 2B-G (0.5 μM – 4.0 μM HRas or Rab proteins; the protein-to-lipid molar ratios, 1:1000 – 1:125). Indeed, HRas had little membrane tethering potency, giving no significant increase in the turbidity of liposomes when assayed even at the highest HRas protein concentrations of 4.0 μM (HRas-to-lipid, 1:125) (Figure 3B). Nevertheless, both of the non-endosomal Rab GTPases tested, Rab1a and Rab3a, retained the intrinsic capacity to directly induce efficient membrane tethering of synthetic liposomes (Figure 3C,D), as shown earlier with six endosomal Rabs in Figure 2. It should be noted that the difference of the *in vitro* membrane tethering potency between different Rab-family members and also between Rab proteins and HRas is not simply relied on their attachment to liposomal membranes in the tethering reactions (Figure 4). To examine the membrane association of Rab and HRas proteins in the current reconstitution systems, liposome co-sedimentation assays

were employed (Figure 4A) with the same experimental conditions as in the liposome turbidity assays (Figure 2, Figure 3; protein-to-lipid, 1:500), demonstrating that all the tested Rab-family and HRas proteins bound were able to comparably and stably bind to liposomal membranes (Figure 4B,C,D,E,F,G,H,I,J). Thus, our data from the turbidity assays (Figure 2, Figure 3) suggest that the intrinsic potency to physically tether two apposed membranes is selectively encoded in the Rab-family members among the Ras-superfamily GTPases and likely to be fully conserved through all the Rab-family members functioning in the endocytic and secretory pathways.

To further confirm the intrinsic membrane tethering capacity of Rab-family GTPases as their genuine function, we employed fluorescence microscopic observations of the reconstituted reactions of Rab-mediated membrane tethering (Figure 5). The tethering reactions were incubated with rhodamine (Rh)-labeled fluorescent liposomes (0.5 mM lipids; 1000 nm diameter) and Rab-family or HRas proteins (4 μM proteins; protein-to-lipid, 1:125) (Figure 5A) as in the liposome turbidity assays (Figure 2; Figure 3). Strikingly, whereas only small particles of non-tethered liposomes were observed when incubated in the absence of any Rab proteins (Figure 5B,C) or with the control HRas protein (Figure 5T,U), all of the tested endosomal and non-endosomal Rab proteins (Rab4a, Rab5a, Rab7a, Rab9a, Rab11a, Rab14, Rab1a, and Rab3a) were able to specifically induce the formation of substantial massive clusters of liposomes (Figure 5D-S). Liposome clusters observed in the fluorescence images were then quantitatively analyzed for the particle size distributions (Figure 6A), yielding the average sizes of Rab-mediated liposome clusters ranging from 7.8 μm^2 to 55 μm^2, which are much larger than those of the control reactions (0.92 μm^2 and 0.80 μm^2 for the reactions without any Rabs and with HRas, respectively) (Figure 6B). These our morphological analyses of Rab-mediated membrane tethering reactions by fluorescence microscopy were fully consistent with the results obtained in the liposome turbidity

assays (Figure 2; Figure 3), thus further establishing the working model that Rab-family proteins themselves can be a *bona fide* membrane tether to directly and physically link two distinct lipid bilayers of subcellular membranes in intracellular membrane tethering.

Class V myosins, the Rab11a effectors, strongly and selectively promote membrane tethering mediated by the cognate Rab GTPase

By comprehensively and quantitatively characterizing *in vitro* membrane tethering reactions reconstituted with chemically defined lipid bilayers and purified recombinant proteins of eight Rab GTPases in human (Rab1a, Rab3a, Rab4a, Rab5a, Rab7a, Rab9a, Rab11a, and Rab14) (Figure 1; Figure 2; Figure 3; Figure 4; Figure 5; Figure 6), we now establish that Rab-family proteins genuinely have the intrinsic potency to directly and specifically tether two distinct lipid bilayers together in the context of a physiologically relevant function. Nevertheless, it is noteworthy that there appears to be wide variability in the tethering capacity of human Rab-family GTPases, although Rab proteins share the highly conserved amino acid sequences and tertiary structures for their Ras-superfamily GTPase domains (Figure 1A; Figure 1 – figure supplement 1) (**Rojas et al., 2012**; **Khan and Ménétrey, 2013**), which exhibited comparable GTP-hydrolysis activities for all the eight Rabs tested (Figure 1C). For typical instances of variability in the Rab-mediated tethering potency, Rab5a and Rab7a were able to trigger rapid membrane tethering at the protein-to-lipid molar ratios of 1:500 (Figure 2C,D, black bold lines), whereas most of the other Rabs (Rab1a, Rab4a, Rab9a, Rab11a, and Rab14) showed little or no tethering activity under the same conditions of the Rab density on the membrane surface (Rab-to-lipid, 1:500) (Figure 2B,E,F,G, black bold lines; Figure 3C, black bold lines). These results led us to hypothesize that (i) the intrinsic tethering activity of Rab proteins is negatively autoregulated in general, especially in the case of the Rabs that cause very slow and inefficient membrane tethering by themselves (Rab1a,

241 Rab4a, Rab9a, Rab11a, and Rab14) and thus (ii) specific Rab-interacting proteins (Rab effectors)
242 drastically enhance the capacity of their cognate Rabs to drive membrane tethering. To test this
243 hypothesis, we next attempted to reconstitute membrane tethering reactions with Rab11a, which
244 had exhibited the lowest tethering potency among the eight Rabs tested in the earlier liposome
245 turbidity assays (Figure 2F), and the cognate Rab11a effectors, class V myosin motor proteins
246 (Myo5A and Myo5B) (Figure 7). Although any Rab11a effectors identified, except for the
247 Exoc6/Sec15 exocyst subunit (**Zhang et al., 2004**; **Wu et al., 2005**; **Wu and Guo, 2015**), have never
248 been proposed or reported to be directly involved in membrane tethering events (**Stenmark,**
249 **2009**; **Hutagalung and Novick, 2011**; **Wandinger-Ness and Zerial, 2014**), it has been thought that,
250 as Rab effectors, class V myosins directly bind and cooperate with the cognate Rab11a on
251 transport vesicles to regulate the specificity of membrane trafficking (**Lapierre et al., 2001**;
252 **Hammer and Wu, 2002**; **Hammer and Sellers, 2012**; **Lindsay et al., 2013**).
253
254 To reconstitute the Rab11a- and class V myosin-dependent membrane tethering reaction in a
255 chemically defined system, we purified the globular tail domains of class V myosin proteins
256 (Myo5A-GTD and Myo5B-GTD) in human, which correspond to the C-terminal residues 1534-1855
257 of myosin 5a (Myo5A) and the residues 1526-1848 of myosin 5b (Myo5B) (Figure 7A,B). It should
258 be noted that previous biochemical and structural studies indicated that these globular tail
259 domains of Myo5A and Myo5B were necessary and sufficient for binding to Rab11a (Figure 7A)
260 (**Roland et al., 2011**; **Lindsay et al., 2013**; **Pylypenko et al., 2013**; **Pylypenko et al., 2016**). Using
261 purified Myo5A-GTD and Myo5B-GTD proteins (Figure 7B), we employed liposome turbidity
262 assays to test whether class V myosin proteins have an effect on membrane tethering reactions
263 mediated by the cognate Rab11a (Figure 7C,D,E). Strikingly, Rab11a-mediated tethering was
264 strongly promoted by addition of an equimolar amount (1 μM) or a 2-fold molar excess (2 μM) of

Myo5A-GTD (Figure 7D) or Myo5B-GTD (Figure 7E) over Rab11a (1 μM; Rab-to-lipid ratio, 1:500), exhibiting much higher initial rates of the turbidity increase than those in the absence of Myo5-GTD proteins. Morphological changes of liposomes in the tethering reactions with Rab11a and Myo5-GTDs were also analyzed by fluorescence microscopy (Figure 7F,G,H,I,J,K), indicating that Rab11a and Myo5-GTD proteins synergistically and specifically induced the formation of massive clusters of liposomes (Figure 7J,K). Thus, the current results from these two independent assays in a chemically defined system uncover the novel function of class V myosins to directly support membrane tethering mediated by their cognate Rab11a GTPase.

Since class V myosins are recognized as Rab effectors that, in general, selectively interact with the GTP-bound from of Rab proteins (**Hammer and Sellers, 2012**), we next tested the guanine nucleotide dependence of Rab11a- and Myo5-GTD-mediated membrane tethering by employing the liposome turbidity assays (Figure 8A). Indeed, the addition of GTP (1 mM) drastically stimulated the synergistic action of Rab11a and Myo5A-GTD (Figure 8B, blue lines) or Myo5B-GTD (Figure 8C, blue lines) upon driving rapid membrane tethering, but the presence of GTP had no effect on the tethering reactions bearing either Rab11a or Myo5-GTD proteins alone (Figure 8B,C, black and red lines). This direct stimulation by GTP on Rab11a/Myo5-GTD-dependent membrane tethering was shown as a very specific effect when added the variable GTP concentrations ranging from 1 μM to 1 mM (Figure 8D,E) and assayed with the other guanine nucleotides, GDP and GTPγS (Figure 8F,G). Our data therefore reflect that Myo5-GTD proteins greatly enhance the tethering activity of Rab11a in a GTP-dependent manner, suggesting that the direct and stable interactions of Myo5-GTD proteins with membrane-bound Rab11a-GTP proteins are required for facilitating membrane tethering. To experimentally test the association of Myo5-GTD proteins with Rab11a proteins on liposomal membranes, liposome co-sedimentation assays were performed under the

289 typical conditions used for the turbidity assays in Figure 8 (Rab-to-lipid ratio, 1:500; Rab-to-Myo5-
290 GTD ratio, 1:1; 1 mM GTP) (Figure 9A). However, we found that the amounts of Myo5A-GTD
291 (Figure 9B, ppt) and Myo5B-GTD (Figure 9E, ppt) bound to and co-isolated with Rab11a-attached
292 liposomes were comparable to those of the control reactions with protein-free liposomes in the
293 absence of Rab11a-His12 (Figure 9C,F, ppt) or in the presence of untagged Rab11a lacking a His12
294 tag (Figure 9D,G, ppt). This indicates, unexpectedly, that the membrane association of Myo5-GTD
295 proteins was not significantly promoted by the recruitment of Rab11a on a liposomal membrane
296 surface. Considering that rapid and efficient Rab11a-mediated membrane tethering is definitely
297 relied on the presence of Myo5-GTD proteins and GTP in the current reconstitution system (Figure
298 7; Figure 8), our results from the co-sedimentation assays (Figure 9) may imply that the transient
299 interactions between Rab11a and Myo5-GTD proteins on a membrane surface are essential for
300 cooperatively accelerating membrane tethering reactions.
301
302 Our current studies have uncovered the novel function of class V myosins to directly promote
303 membrane tethering mediated by their cognate Rab11a GTPase in a GTP-dependent manner, by
304 thoroughly characterizing reconstituted membrane tethering in the chemically defined systems
305 with purified Rab11a and Myo5-GTD proteins (Figure 7; Figure 8; Figure 9). However, it could still
306 be argued that Myo5-GTD proteins can non-physiologically induce tethering or aggregation of
307 liposomal membranes coated by other non-cognate Rab-His12 proteins or even coated by any
308 types of soluble proteins modified with a polyhistidine tag. In this context, to more strictly validate
309 the specificity of Rab11a/Myo5-GTD-dependent membrane tethering, we further explored the
310 liposome turbidity assays in the presence of Myo5-GTD proteins (Figure 10A), not only for the
311 cognate Rab11a but also for the other four Rab proteins including Rab1a, Rab4a, Rab9a, and
312 Rab14, which had shown relatively slow and inefficient membrane tethering by themselves,

similar to Rab11a (Figure 2; Figure 3). Although Rab11a and either Myo5A-GTD or Myo5B-GTD proteins synergistically triggered very rapid and efficient membrane tethering (Figure 10B,C, blue lines), fully consistent with the earlier results in Figure 8, these Myo5-GTD proteins indeed had only minor or little effect on the tethering potency of Rab1a, Rab4a, Rab9a, and Rab14 (Figure 10B,C, green, black, cyan, and red lines). Thus, our data faithfully reflect that both Myo5A-GTD and Myo5B-GTD recognize and act upon exclusively the cognate Rab11a at the membrane surface of lipid bilayers, thereby selectively activating Rab11a-mediated membrane tethering reactions. The current findings from reconstituted membrane tethering with purified Rab and Myo5-GTD proteins (Figure 7; Figure 8; Figure 9; Figure 10) provide new insights into how Rab GTPases on subcellular membranes (transport vesicles, organelle membranes, or the plasma membrane) and class V myosin motors on actin cytoskeletal tracks cooperate with each other to promote membrane tethering and how their functions synergistically contribute to the spatiotemporal specificity of membrane tethering and beyond.

Conclusions

Membrane tethering is one of the most critical and important processes to determine the specificity of membrane traffic in eukaryotic endomembrane systems, delivering the correct sets of cargoes (proteins, lipids, etc.) to the correct locations (organelles, the plasma membrane, the extracellular space, etc.) (**Waters and Pfeffer, 1999**). From a large body of prior studies using genetic, cell biological, biochemical, and structural biological approaches on this essential membrane tethering process, we generally recognize that a number of diverse but specific types of “Rab effectors” have been described as the so-called “tethering factors”, such as coiled-coil tethering proteins and multisubunit tethering complexes (**Yu and Hughson, 2010**; **Chia and Gleeson, 2014**; **Kuhlee et al., 2015**). However, for the most cases, it remains ambiguous indeed

whether these "tethering factors" identified are a *bona fide* membrane tether that physically links two distinct opposing membranes by itself or, furthermore, whether they are even involved directly in membrane tethering events (**Brunet and Sacher, 2014**). In this context, in order to thoroughly define and characterize the molecular functions in membrane tethering for Rab-family GTPases and class V myosin cytoskeletal motor proteins as the specific Rab effectors, we have undertaken to recapitulate the membrane tethering machinery in the chemically defined systems reconstituted with synthetic lipid bilayers of liposomes and purified proteins of human Rab GTPases and class V myosins (**Figure 1**; **Figure 2**; **Figure 7**).

Our current *in vitro* reconstitution studies present three new findings supporting the working model of intracellular membrane tethering mediated by Rab-family GTPases as a genuine membrane tether: (1) All the eight Rab proteins tested, including both endosomal and non-endosomal Rabs, have the intrinsic capacity to physically tether two apposed membranes under the experimental conditions mimicking the lipid composition and Rab density of subcellular organelles/vesicles in mammalian cells, establishing the conserved tethering function of the Rab-family members (**Figure 2**; **Figure 3**; **Figure 5**). (2) The tethering capacity of Rab proteins is a specific function among the Ras superfamily GTPases and yet highly variable for each of different Rab proteins (**Figure 2**; **Figure 3**; **Figure 5**). This suggests that the Rab subfamily-specific (RabSF) motifs could be the regions responsible for controlling the membrane tethering potency of each Rab (**Pereira-Leal and Seabra, 2000**; **Stein et al., 2012**). Finally, (3) the Rab effectors, class V myosins, can drastically and specifically promote membrane tethering mediated by their cognate Rab GTPase, Rab11a, in a GTP-dependent manner (**Figure 7**; **Figure 8**; **Figure 10**). This finding leads us to hypothesize that cytoskeletal motor proteins, including class V myosins and also microtubule-based motor proteins, act as "tethering factors" (not "tethers") that directly and

positively regulate Rab-mediated membrane tethering (**Hammer and Wu, 2002**; **Akhmanova and Hammer, 2010**). Understanding a detailed picture of the protein machinery of Rab-mediated membrane tethering will need further studies using a chemically defined reconstitution system, which may focus on testing tethering by the heterotypic Rab combinations, determining the specific regions in Rab molecules responsible for tethering, and reconstituting Rab-mediated tethering in the presence of different types of Rab effectors.

Materials and methods

Protein expression and purification

The coding sequences for the eight isoforms of Rab-family GTPases (Rab1a, Rab3a, Rab4a, Rab5a, Rab7a, Rab9a, Rab11a, and Rab14) in human and for human HRas GTPase were amplified by polymerase chain reaction (PCR) with Human Universal QUICK-Clone cDNA II (Clontech, Mountain View, CA) as a template cDNA and KOD-Plus-Neo DNA polymerase (Toyobo, Osaka, Japan), as described (**Tamura and Mima, 2014**). The amplified PCR fragments contained the sequence encoding a human rhinovirus (HRV) 3C protease site (Leu-Glu-Val-Leu-Phe-Gln-Gly-Pro) upstream of the initial ATG codons and the sequence encoding polyhistidine residues (His12) downstream of the codons for a C-terminal residue, yielding the full-length Rab and HRas proteins with three extra N-terminal residues (Gly-Pro-Gly) and a C-terminal His12 tag after HRV 3C protease cleavage. For Rab11a, the PCR fragment without the polyhistidine-coding sequence was also amplified as above, to prepare the Rab11a protein lacking the C-terminal His12 tag (untagged Rab11a). All of these PCR fragments for the Rab-family and HRas GTPases were inserted into a pET-41 Ek/LIC vector (Novagen, Madison, WI), which is designed to express an N-terminal GST-His6-tagged protein, by the ligation-independent cloning method (Novagen).

Recombinant Rab and HRas proteins were expressed in the *Escherichia coli* BL21(DE3) cells (Novagen) harboring the pET-41-based vectors in Lysogeny Broth (LB) medium (1 liter each) with kanamycin (50 μg/ml) by induction with 0.1 mM IPTG at 37°C for 3 hours. *E. coli* cells harvested after IPTG induction were resuspended in 40 ml each of RB150 (20 mM Hepes-NaOH, pH 7.4, 150 mM NaCl, 10% glycerol) containing 0.1 mM GTP, 5mM $MgCl_2$, 1 mM DTT, 1 mM PMSF, and 1.0 μg/ml pepstatin A, freeze-thawed in a liquid nitrogen and a water bath at 30°C, lysed by sonication using UD-201 ultrasonic disrupter (Tomy Seiko, Tokyo, Japan), and then ultracentrifuged at 50,000

392 rpm for 75 min at 4°C with a 70 Ti rotor (Beckman Coulter, Indianapolis, IN). The supernatants
393 obtained were mixed with COSMOGEL GST-Accept beads (50% slurry, 4 ml each; Nacalai Tesque,
394 Kyoto, Japan) and were incubated at 4°C for 2 hours with gentle agitation to isolate GST-His6-
395 tagged Rab-His12 and HRas-His12 proteins. The protein-bound GST-Accept beads were washed
396 four times in RB150 containing 5 mM $MgCl_2$ and 1 mM DTT (8 ml each), resuspended in the same
397 buffer (4 ml each), supplemented with HRV 3C protease (4 units/ml final; Novagen), and incubated
398 without agitation (4°C, 16 hours) to cleave off and elute Rab-His12 and HRas-His12 proteins. After
399 centrifugation of the bead suspensions (15,300 g, 10 min, 4°C), purified Rab-His12 and HRas-His12
400 proteins were harvested from the supernatants.
401
402 For class V myosins, the coding sequences of the globular tail domains of human myosin 5a
403 (Myo5A-GTD; residues 1534-1855) and myosin 5b (Myo5B-GTD; residues 1526-1848) with the
404 sequence encoding a HRV 3C-protease site upstream of the initial codons were amplified by PCR
405 as above and then cloned into a pET-30 Ek/LIC vector (Novagen) expressing an N-terminal His6-
406 tagged protein. Recombinant Myo5A-GTD (1534-1855) and Myo5B-GTD (1526-1848) proteins
407 were expressed in the *E. coli* BL21(DE3) cells harboring the pET-30-based vectors in LB medium
408 with kanamycin (1 liter each) by induction with 0.1 mM IPTG (16°C, 16 hours). *E. coli* cells were
409 resuspended in 40 ml each of RB150 containing $MgCl_2$ (5 mM), DTT (1 mM), PMSF (1 mM), and
410 pepstatin A (1.0 μg/ml), followed by freeze-thaw treatment, sonication, and ultracentrifugation as
411 above. The supernatants were mixed with Complete His-Tag Purification Resin beads (50% slurry,
412 4 ml each; Roche, Basel, Switzerland) and were incubated at 4°C for 2 hours with gentle agitation
413 to isolate His6-tagged Myo5A-GTD and Myo5B-GTD proteins. The protein-bound beads were
414 washed four times in RB150 containing 5 mM $MgCl_2$, 1 mM DTT, and 20 mM imidazole (8 ml each),
415 resuspended in the same buffer (2 ml each) containing HRV 3C protease (15 units/ml; Novagen),

and incubated with gentle agitation (4°C, 16 hours). After centrifugation of the bead suspensions (15,300 g, 10 min, 4°C), purified Myo5A-GTD and Myo5B-GTD proteins, which had been cleaved off from the beads, were harvested from the supernatants and dialyzed against RB150 containing 5 mM $MgCl_2$ and 1 mM DTT.

GTPase activity assay

GTP-hydrolysis activities of human Rab-family and HRas GTPases were assayed by quantitating released free phosphate molecules during the hydrolytic reactions, using the Malachite Green-based reagent Biomol Green (Enzo Life Sciences, Farmingdale, NY) as described (**Tamura and Mima, 2014**; **Sugiura and Mima, 2016**), with modifications. Purified recombinant Rab-family and HRas proteins (2 μM final) were incubated at 30°C for 1 hour in RB150 containing 6 mM $MgCl_2$, 1 mM DTT, and 1 mM GTP or GTPγS. After a 1-hour incubation, the reaction mixtures (50 μl each) were supplemented with the Biomol Green reagent (50 μl each), further incubated at 30°C for 30 min, and measured for absorbance at 620 nm in a clear 96-well microplate (Falcon no. 351172; Corning, Corning, NY) using the SpectraMax Paradigm plate reader with the ABS-MONO cartridge (Molecular Devices, Sunnyvale, CA). All of the data obtained were corrected by subtracting the absorbance values of the control reactions without any Rab and HRas GTPases. To calculate the concentrations of released phosphate molecules in the reactions, phosphate standard samples (2.5 – 160 μM final; Enzo Life Sciences) were also incubated and assayed using the same protocol. Means and standard deviations of the specific GTPase activities for purified Rab-family and HRas proteins (μM phosphate/min/μM protein) were determined from three independent experiments.

Liposome preparation

All of the non-fluorescent lipids were purchased from Avanti Polar Lipids (Alabaster, AL).

Fluorescent lipids, Rh-PE and FL-PE, were obtained from Molecular Probes (Eugene, OR). Lipid mixes for the Rh-labeled liposomes used in liposome turbidity assays, fluorescence microscopy, and liposome co-sedimentation assays contained 1-palmitoyl-2-oleoyl-PC (POPC) [42% (mol/mol)], POPE (16.5%), soy PI (10%), POPS (5%), cholesterol (20%), DOGS-NTA (6%), and Rh-PE (0.5%). Dried lipid films harboring the physiological mimic lipid composition (**van Meer et al., 2008**; **Tamura and Mima, 2014**) were completely resuspended in RB150 containing 5 mM $MgCl_2$ and 1 mM DTT by vortexing, yielding 8 mM total lipids in final, then incubated at 37°C for 1 hour with shaking, freeze-thawed in liquid N_2 and a water bath at 30°C, and extruded 21 times through polycarbonate filters (pore diameter, 400 or 1000 nm; Avanti Polar Lipids) in a mini-extruder (Avanti Polar Lipids) at 40°C. Lipid concentrations of the extruded liposomes were determined from the fluorescence of Rh-PE (λex = 550 nm, λem = 590 nm) and FL-PE (λex = 486 nm, λem = 529 nm) using the SpectraMax Paradigm plate reader with the TUNE cartridge (Molecular Devices) and a black 384-well plate (Corning no. 3676; Corning). Liposome solutions were diluted with RB150 containing 5 mM $MgCl_2$ and 1 mM DTT to 5 mM total lipids in final and stored at 4°C.

Liposome turbidity assay

Membrane tethering of Rab GTPase-anchored liposomes was monitored by turbidity changes of liposome solutions as described (**Ohki et al., 1982**; **Hui et al., 2011**; **Tamura and Mima, 2014**; **Liu et al., 2015**), with modifications. After preincubating liposome suspensions and Rab protein solutions separately at 30°C for 10 min, liposomes (400 nm diameter; 0.5 mM total lipids in final) were mixed with Rab proteins (0.5 – 4.0 μM in final) in RB150 containing 5 mM $MgCl_2$ and 1 mM DTT (total 150 μl for each), immediately followed by measuring the absorbance changes of the liposome suspensions at 400 nm in a DU720 spectrophotometer (Beckman Coulter) at room temperature for 300 sec. For the assays with class V myosins, Rab proteins (1 μM final) were

464 preincubated at 30°C for 30 min in the presence of Myo5A-GTD or Myo5B-GTD (0.5 – 2.0 μM final)
465 before mixing with liposomes. All liposome turbidity data were obtained from one experiment
466 and were typical of those from more than three independent experiments.
467
468 **Liposome co-sedimentation assay**
469 Rh-labeled liposome suspensions (400 nm diameter; 1 mM total lipids in final) were mixed with
470 purified Rab, HRas, or BSA proteins (2 μM in final) in RB150 containing 5 mM $MgCl_2$ and 1 mM DTT
471 (100 μl each) and subsequently incubated at 30°C for 30 min. For the experiments with class V
472 myosins, the reaction mixtures were further supplemented with GTP (1 mM final) and Myo5A-
473 GTD or Myo5B-GTD (2 μM final). After incubation, these reactions were ultracentrifuged at 50,000
474 rpm for 30 min at 4°C with a TLA100 rotor and an Optima TLX ultracentrifuge (Beckman Coulter).
475 The pellets and supernatants obtained were analyzed by SDS-PAGE and Coomassie Blue staining.
476
477 **Fluorescence microscopy**
478 After separately preincubating liposome suspensions and Rab protein solutions at 30°C for 10 or
479 30 min, liposomes (1000 nm diameter; 0.5 or 0.8 mM total lipids in final) and Rab proteins (3.0 or
480 4.0 μM final) were mixed in RB150 containing 5 mM $MgCl_2$ and 1 mM DTT (total 50 μl for each),
481 further incubated at 30°C for 30 min or 1 hour, transferred to ice, and subjected to fluorescence
482 microscopy. For the reactions with class V myosins, Rab11a-His12 (3 μM final) was preincubated
483 in the presence of Myo5A-GTD or Myo5B-GTD (3 μM final) at 30°C for 30 min before incubating
484 with liposomes. A drop of the incubated reactions (5 μl each) was placed on a microscope slide
485 (S2111; Matsunami Glass, Kishiwada, Japan) and covered with an 18-mm coverslip (Matsunami
486 Glass). Fluorescence microscopy was performed using a BZ-9000 fluorescence microscope
487 (Keyence, Osaka, Japan) equipped with Plan Apo 40X NA 0.95 and Plan Apo VC 100X NA 1.40 oil

488 objective lenses (Nikon, Tokyo, Japan) and TRITC and GFP-BP filters (Keyence). Digital images
489 obtained were processed using the BZ-II viewer application (Keyence) and the ImageJ2 software
490 (National Institutes of Health, Bethesda, MD). Particle sizes of Rab-mediated liposome clusters
491 were measured using ImageJ2 after setting the lower intensity threshold level to 100 and the
492 upper intensity threshold level to 255 (**Stroupe et al., 2009**; **Hickey and Wickner, 2010**).
493

Acknowledgements

We thank Dr. Naoki Tamura (Institute for Protein Research, Osaka University; now Fukushima Medical University School of Medicine) for valuable suggestions on this project and for substantial contributions to preparing the expression vectors for human Rab GTPases. We are grateful to Drs. Junichi Takagi and Yukiko Matsunaga (Institute for Protein Research, Osaka University) for access to fluorescence microscopy experiments. This study was in part supported by the Program to Disseminate Tenure Tracking System from the Ministry of Education, Culture, Sports, Science and Technology, Japan (MEXT) and Grants-in-Aid for Scientific Research from MEXT (to JM).

Author contributions

JM designed the research; JM and MI performed the experiments; JM and MI analyzed the data; JM wrote the manuscript.

References

Akhmanova A, Hammer JA 3rd. 2010. Linking molecular motors to membrane cargo. *Current Opinion in Cell Biology* **22**:479-487.
doi: 10.1016/j.ceb.2010.04.008

Baker RW, Hughson FM. 2016. Chaperoning SNARE assembly and disassembly. *Nature Reviews Molecular Cell Biology* **17**:465-479.
doi: 10.1038/nrm.2016.65

Bonifacino JS, Glick BS. 2004. The mechanisms of vesicle budding and fusion. *Cell* **116**:153-166.
doi: 10.1016/S0092-8674(03)01079-1

Brunet S, Sacher M. 2014. Are all multisubunit tethering complexes bona fide tethers? *Traffic* **15**:1282-1287.
doi: 10.1111/tra.12200

Cai H, Reinisch K, Ferro-Novick S. 2007. Coats, tethers, Rabs, and SNAREs work together to mediate the intracellular destination of a transport vesicle. *Developmental Cell* **12**:671-682.
doi: 10.1016/j.devcel.2007.04.005

Cheung PY, Limouse C, Mabuchi H, Pfeffer SR. 2015. Protein flexibility is required for vesicle tethering at the Golgi. *eLife* **4**:e12790.
doi: 10.7554/eLife.12790

Chia PZ, Gleeson PA. 2014. Membrane tethering. *F1000Prime Reports* **6**:74.
doi: 10.12703/P6-74

Erickson HP. 2009. Size and shape of protein molecules at the nanometer level determined by sedimentation, gel filtration, and electron microscopy. *Biological Procedures Online* **11**:32-51.
doi: 10.1007/s12575-009-9008-x

Furukawa N, Mima J. 2014. Multiple and distinct strategies of yeast SNAREs to confer the specificity of membrane fusion. *Scientific Reports* **4**:4277.
doi: 10.1038/srep04277

Grosshans BL, Ortiz D, Novick P. 2006. Rabs and their effectors: achieving specificity in membrane traffic. *Proceedings of the National Academy of Sciences of USA* **103**:11821-11827.
doi: 10.1073/pnas.0601617103

Hammer JA 3rd, Sellers JR. 2012. Walking to work: roles for class V myosins as cargo transporters. *Nature Reviews Molecular Cell Biology* **13**:13-26.
doi: 10.1038/nrm3248

Hammer JA 3rd, Wu XS. 2002. Rabs grab motors: defining the connections between Rab GTPases and motor proteins. *Current Opinion in Cell Biology* **14**:69-75.
doi: 10.1016/S0955-0674(01)00296-4

553
554 **Hickey CM**, Wickner W. 2010. HOPS initiates vacuole docking by tethering membranes before
555 trans-SNARE complex assembly. *Molecular Biology of the Cell* **21**:2297-2305.
556 doi: 10.1091/mbc.E10-01-0044
557
558 **Ho R**, Stroupe C. 2015. The HOPS/class C Vps complex tethers membranes by binding to one Rab
559 GTPase in each apposed membrane. *Molecular Biology of the Cell* **26**:2655-2663.
560 doi: 10.1091/mbc.E14-04-0922
561
562 **Ho R**, Stroupe C. 2016. The HOPS/class C Vps complex tethers high-curvature membranes via a
563 direct protein-membrane interaction. *Traffic* **17**:1078-1090.
564 doi: 10.1111/tra.12421
565
566 **Hui E**, Gaffaney JD, Wang Z, Johnson CP, Evans CS, Chapman ER. 2011. Mechanism and function of
567 synaptotagmin-mediated membrane apposition. *Nature Structural & Molecular Biology* **18**:813-
568 821.
569 doi: 10.1038/nsmb.2075
570
571 **Hutagalung AH**, Novick PJ. 2011. Role of Rab GTPases in membrane traffic and cell physiology.
572 *Physiological Reviews* **91**:119-149.
573 doi: 10.1152/physrev.00059.2009
574
575 **Izawa R**, Onoue T, Furukawa N, Mima J. 2012. Distinct contributions of vacuolar Qabc- and R-
576 SNARE proteins to membrane fusion specificity. *The Journal of Biological Chemistry* **287**:3445-
577 3453.
578 doi: 10.1074/jbc.M111.307439
579
580 **Jahn R**, Scheller RH. 2006. SNAREs--engines for membrane fusion. *Nature Reviews Molecular Cell*
581 *Biology* **7**:631-643.
582 doi: 10.1038/nrm2002
583
584 **Khan AR**, Ménétrey J. 2013. Structural biology of Arf and Rab GTPases' effector recruitment and
585 specificity. *Structure* **21**:1284-1297.
586 doi: 10.1016/j.str.2013.06.016
587
588 **Kuhlee A**, Raunser S, Ungermann C. 2015. Functional homologies in vesicle tethering. *FEBS Letters*
589 **589**:2487-2497.
590 doi: 10.1016/j.febslet.2015.06.001
591
592 **Lapierre LA**, Kumar R, Hales CM, Navarre J, Bhartur SG, Burnette JO, Provance DW Jr, Mercer JA,
593 Bähler M, Goldenring JR. 2001. Myosin Vb is associated with plasma membrane recycling systems.
594 *Molecular Biology of the Cell* **12**:1843-1857.
595 doi: 10.1091/mbc.12.6.1843
596
597 **Lindsay AJ**, Jollivet F, Horgan CP, Khan AR, Raposo G, McCaffrey MW, Goud B. 2013. Identification
598 and characterization of multiple novel Rab-myosin Va interactions. *Molecular Biology of the Cell*
599 **24**:3420-3434.
600 doi: 10.1091/mbc.E13-05-0236

Liu TY, Bian X, Romano FB, Shemesh T, Rapoport TA, Hu J. 2015. Cis and trans interactions between atlastin molecules during membrane fusion. *Proceedings of the National Academy of Sciences of USA* **112**:E1851-E1860.
doi: 10.1073/pnas.1504368112

Lo SY, Brett CL, Plemel RL, Vignali M, Fields S, Gonen T, Merz AJ. 2012. Intrinsic tethering activity of endosomal Rab proteins. *Nature Structural & Molecular Biology* **19**:40-47.
doi: 10.1038/nsmb.2162

McNew JA, Parlati F, Fukuda R, Johnston RJ, Paz K, Paumet F, Söllner TH, Rothman JE. 2000. Compartmental specificity of cellular membrane fusion encoded in SNARE proteins. *Nature* **407**:153-159.
doi: 10.1038/35025000

Murray DH, Jahnel M, Lauer J, Avellaneda MJ, Brouilly N, Cezanne A, Morales-Navarrete H, Perini ED, Ferguson C, Lupas AN, Kalaidzidis Y, Parton RG, Grill SW, Zerial M. 2016. An endosomal tether undergoes an entropic collapse to bring vesicles together. *Nature* **537**:107-111.
doi: 10.1038/nature19326

Nagle JF, Tristram-Nagle S. 2000. Structure of lipid bilayers. *Biochimica et Biophysica Acta* **1469**:159-195.
doi: 10.1016/S0304-4157(00)00016-2

Ohki S, Düzgüneş N, Leonards K. 1982. Phospholipid vesicle aggregation: effect of monovalent and divalent ions. *Biochemistry* **21**:2127-2133.
doi: 10.1021/bi00538a022

Parlati F, Varlamov O, Paz K, McNew JA, Hurtado D, Söllner TH, Rothman JE. 2002. Distinct SNARE complexes mediating membrane fusion in Golgi transport based on combinatorial specificity. *Proceedings of the National Academy of Sciences of USA* **99**:5424-5429.
doi: 10.1073/pnas.082100899

Pereira-Leal JB, Seabra MC. 2000. The mammalian Rab family of small GTPases: definition of family and subfamily sequence motifs suggests a mechanism for functional specificity in the Ras superfamily. *Journal of Molecular Biology* **301**:1077-1087.
doi: 10.1006/jmbi.2000.4010

Pylypenko O, Attanda W, Gauquelin C, Lahmani M, Coulibaly D, Baron B, Hoos S, Titus MA, England P, Houdusse AM. 2013. Structural basis of myosin V Rab GTPase-dependent cargo recognition. *Proceedings of the National Academy of Sciences of USA* **110**:20443-20448.
doi: 10.1073/pnas.1314329110

Pylypenko O, Welz T, Tittel J, Kollmar M, Chardon F, Malherbe G, Weiss S, Michel CI, Samol-Wolf A, Grasskamp AT, Hume A, Goud B, Baron B, England P, Titus MA, Schwille P, Weidemann T, Houdusse A, Kerkhoff E. 2016. Coordinated recruitment of Spir actin nucleators and myosin V motors to Rab11 vesicle membranes. *eLife* **5**:e17523.
doi: 10.7554/eLife.17523

649
650 **Rojas AM**, Fuentes G, Rausell A, Valencia A. 2012. The Ras protein superfamily: evolutionary tree
651 and role of conserved amino acids. *The Journal of Cell Biology* **196**:189-201.
652 doi: 10.1083/jcb.201103008
653
654 **Roland JT**, Bryant DM, Datta A, Itzen A, Mostov KE, Goldenring JR. 2011. Rab GTPase-Myo5B
655 complexes control membrane recycling and epithelial polarization. *Proceedings of the National*
656 *Academy of Sciences of USA* **108**:2789-2794.
657 doi: 10.1073/pnas.1010754108
658
659 **Scales SJ**, Chen YA, Yoo BY, Patel SM, Doung YC, Scheller RH. 2000. SNAREs contribute to the
660 specificity of membrane fusion. *Neuron* **26**:457-464.
661 doi: 10.1016/S0896-6273(00)81177-0
662
663 **Stein M**, Pilli M, Bernauer S, Habermann BH, Zerial M, Wade RC. 2012. The interaction properties
664 of the human Rab GTPase family--comparative analysis reveals determinants of molecular binding
665 selectivity. *PLoS One* **7**:e34870.
666 doi: 10.1371/journal.pone.0034870
667
668 **Stenmark H**. 2009. Rab GTPases as coordinators of vesicle traffic. *Nature Reviews Molecular Cell*
669 *Biology* **10**:513-525.
670 doi: 10.1038/nrm2728
671
672 **Stroupe C**, Hickey CM, Mima J, Burfeind AS, Wickner W. 2009. Minimal membrane docking
673 requirements revealed by reconstitution of Rab GTPase-dependent membrane fusion from
674 purified components. *Proceedings of the National Academy of Sciences of USA* **106**:17626-17633.
675 doi: 10.1073/pnas.0903801106
676
677 **Sugiura S**, Mima J. 2016. Physiological lipid composition is vital for homotypic ER membrane fusion
678 mediated by the dynamin-related GTPase Sey1p. *Scientific Reports* **6**:20407.
679 doi: 10.1038/srep20407
680
681 **Takamori S**, Holt M, Stenius K, Lemke EA, Grønborg M, Riedel D, Urlaub H, Schenck S, Brügger B,
682 Ringler P, Müller SA, Rammner B, Gräter F, Hub JS, De Groot BL, Mieskes G, Moriyama Y, Klingauf
683 J, Grubmüller H, Heuser J, Wieland F, Jahn R. 2006. Molecular anatomy of a trafficking organelle.
684 *Cell* **127**:831-846.
685 doi: 10.1016/j.cell.2006.10.030
686
687 **Tamura N**, Mima J. 2014. Membrane-anchored human Rab GTPases directly mediate membrane
688 tethering *in vitro*. *Biology Open* **3**:1108-1115.
689 doi: 10.1242/bio.20149340
690
691 **van Meer G**, Voelker DR, Feigenson GW. 2008. Membrane lipids: where they are and how they
692 behave. *Nature Reviews Molecular Cell Biology* **9**:112-124.
693 doi: 10.1038/nrm2330
694
695 **Wandinger-Ness A**, Zerial M. 2014. Rab proteins and the compartmentalization of the endosomal
696 system. *Cold Spring Harbor Perspectives in Biology* **6**:a022616.

697 doi: 10.1101/cshperspect.a022616
698
699 **Waters MG**, Pfeffer SR. 1999. Membrane tethering in intracellular transport. *Current Opinion in*
700 *Cell Biology* **11**:453-459.
701 doi:10.1016/S0955-0674(99)80065-9
702
703 **Wu B**, Guo W. 2015. The exocyst at a glance. *Journal of Cell Science* **128**:2957-2964.
704 doi: 10.1242/jcs.156398
705
706 **Wu S**, Mehta SQ, Pichaud F, Bellen HJ, Quiocho FA. 2005. Sec15 interacts with Rab11 via a novel
707 domain and affects Rab11 localization in vivo. *Nature Structural Molecular Biology* **12**:879-885.
708 doi: 10.1038/nsmb987
709
710 **Yu IM**, Hughson FM. 2010. Tethering factors as organizers of intracellular vesicular traffic. *Annual*
711 *Review of Cell and Developmental Biology* **26**:137-156.
712 doi: 10.1146/annurev.cellbio.042308.113327
713
714 **Zhang XM**, Ellis S, Sriratana A, Mitchell CA, Rowe T. 2004. Sec15 is an effector for the Rab11 GTPase
715 in mammalian cells. *The Journal of Biological Chemistry* **279**:43027-43034.
716 doi: 10.1074/jbc.M402264200
717

Figure legends

Figure 1. Purification of human Rab GTPases used in this reconstitution study.

(**A**) Schematic representation of the endosomal Rabs (Rab4a, Rab5a, Rab7a, Rab9a, Rab11a, and Rab14), non-endosomal Rabs (Rab1a and Rab3a), and HRas GTPase in human, showing their amino acid residues, domains (Ras-superfamily GTPase domains and hypervariable regions), and intracellular locations, which include early endosome (EE), recycling endosome (RE), plasma membrane (PM), late endosome (LE), lysosome (Ly), endoplasmic reticulum (ER), Golgi, and secretory vesicle (SV).

(**B**) Coomassie Blue-stained gels of purified recombinant proteins of the C-terminally His12-tagged endosomal Rab, non-endosomal Rab, and HRas GTPases and the untagged form of Rab11a used in this study.

(**C**) Intrinsic GTP-hydrolysis activities of purified Rab proteins. Purified Rab-His12, HRas-His12, and untagged Rab11a proteins (2 μM) were incubated at 30°C for 1 h in RB150 containing $MgCl_2$ (6 mM), DTT (1 mM), and GTP (1 mM) or GTPγS (1 mM) for the control, followed by assaying released free phosphate molecules using a Malachite Green-based reagent.

Figure 1 – figure supplement 1. Amino acid sequence alignment of the Rab- and Ras-family GTPases in human used in this study. Multiple alignment of the sequences was performed using Clustal W (http://www.genome.jp/tools/clustalw/) and ESPript 3.0 (http://espript.ibcp.fr/ESPript/ESPript/).

Figure 2. Endosomal Rab GTPases directly initiate membrane tethering by themselves in a chemically defined reconstitution system.

(**A**) Schematic representation of liposome turbidity assays for testing Rab-mediated liposome

742 tethering in **B**-**G**.

743 (**B**-**G**) Endosomal Rab-His12 proteins (0.5 – 4 μM each), Rab4a-His12 (**B**), Rab5a-His12 (**C**), Rab7a-
744 His12 (**D**), Rab9a-His12 (**E**), Rab11a-His12 (**F**), and Rab14-His12 (**G**), were incubated with synthetic
745 liposomes bearing physiological mimic lipid composition (400 nm diameter; 0.5 mM lipids) in
746 RB150 containing $MgCl_2$ (5 mM) and DTT (1 mM) at room temperature for 300 sec. During
747 incubation, turbidity changes of the Rab-liposome mixed reactions were monitored by measuring
748 the absorbance at 400 nm. The protein-to-lipid molar ratios used for these turbidity reactions
749 were from 1:1000 to 1:125, as indicated.

750

751 **Figure 3.** Non-endosomal Rab GTPases have the inherent potency to specifically mediate
752 membrane tethering.

753 (**A**) Schematic representation of liposome turbidity assays for the non-Rab Ras superfamily GTPase,
754 HRas, and non-endosomal Rab GTPases, Rab1a in ER-Golgi traffic and Rab3a in exocytosis, in **B**-**D**.
755 (**B**-**D**) Liposome turbidity assays were employed as in Figure 2B-G, with HRas-His12 (**B**), Rab1a-
756 His12 (**C**), and Rab3a-His12 (**D**) proteins (0.5 – 4 μM each in final) and physiological mimic synthetic
757 liposomes (0.5 mM total lipids in final). The protein-to-lipid molar ratios used were indicated.

758

759 **Figure 4.** Membrane association of Rab-His12 proteins onto DOGS-NTA-bearing liposomes.
760 (**A**) Schematic representation of liposome co-sedimentation assays for testing membrane
761 attachment of Rab-His12 proteins used in Figure 2 and Figure 3.
762 (**B**-**K**) Rh-labeled liposomes (400 nm diameter; 1 mM total lipids in final) were incubated (30°C, 30
763 min) with Rab4a-His12 (**B**), Rab5a-His12 (**C**), Rab7a-His12 (**D**), Rab9a-His12(**E**), Rab11a-His12 (**F**),
764 Rab14-His12 (**G**), Rab1a-His12 (**H**), Rab3a-His12 (**I**), HRas-His12 (**J**), and BSA for a negative control
765 (**K**) (2 μM final for each), and ultracentrifuged (50,000 rpm, 30 min, 4°C). The supernatants (sup)

766 and precipitates (ppt) obtained were analyzed by SDS-PAGE and Coomassie Blue staining.

767

768 **Figure 5.** Rab-mediated membrane tethering induces the formation of massive liposome clusters.

769 (**A**) Schematic representation of fluorescence microscopic observations of Rab-mediated liposome

770 clusters.

771 (**B**-**U**) Fluorescence images (**B**, **D**, **F**, **H**, **J**, **L**, **N**, **P**, **R**, **T**) and bright field images (**C**, **E**, **G**, **I**, **K**, **M**, **O**, **Q**,

772 **S**, **U**) of Rab-mediated liposome clusters. Fluorescently-labeled liposomes bearing Rh-PE (1000

773 nm diameter; 0.5 mM lipids in final) were incubated at 30°C for 1 h, in the absence (**B**, **C**) and

774 presence of the Rab- and Ras-family GTPases (4 μM each in final), including Rab4a-His12 (**D**, **E**),

775 Rab5a-His12 (**F**, **G**), Rab7a-His12 (**H**, **I**), Rab9a-His12 (**J**, **K**), Rab11a-His12 (**L**, **M**), Rab14-His12 (**N**,

776 **O**), Rab1a-His12 (**P**, **Q**), Rab3a-His12 (**R**, **S**), and HRas-His12 (**T**, **U**), and subjected to fluorescence

777 microscopy. Scale bars: 20 μm.

778

779 **Figure 6.** Particle size distributions of liposome clusters induced by Rab-mediated membrane

780 tethering.

781 (**A**) Particle sizes of the Rab-mediated liposome clusters observed in the fluorescence images of

782 Figure 5.

783 (**B**) Particle numbers and average sizes of the Rab-mediated liposome clusters observed in the

784 fluorescence images of Figure 5.

785

786 **Figure 7.** Class V myosin globular tail domains, Myo5A-GTD and Myo5B-GTD, strongly stimulate

787 Rab11a-dependent membrane tethering.

788 (**A**) Schematic representation of class V myosins in human, Myo5A and Myo5B, showing their

789 amino acid residues and domains including myosin motor domains, IQ motifs, coiled coil regions,

and globular tail domains (GTDs). Representative Myo5-interacting Rab GTPases and the Rab-binding regions in Myo5A and Myo5B are indicated.

(**B**) The Coomassie Blue-stained gel of purified Myo5A-GTD and Myo5B-GTD proteins, which are comprised of the amino acid residues 1534-1855 and 1526-1848, respectively.

(**C**) Schematic representation of liposome turbidity assays for testing Rab11a- and Myo5-GTD-dependent liposome tethering in **D**, **E**.

(**D**, **E**) Liposome turbidity assays were employed with Rab11a-His12 (1 μM final) as in Figure 2F, but in the presence of Myo5A-GTD (**D**) and Myo5B-GTD (**E**) (0.5 – 2 μM final).

(**F**-**K**) Fluorescence images of Rab11a-mediated liposome clusters in the presence of Myo5-GTDs. Rab11a-His12 (3 μM final) and Myo5A-GTD or Myo5B-GTD (3 μM final) were preincubated at 30°C for 30 min, mixed with Rh-labeled liposomes (1000 nm diameter; 0.8 mM lipids in final), further incubated (30°C, 30 min), and subjected to fluorescence microscopy (**J**, **K**). For a control, Rab11a-His12, Myo5-GTD, or both were omitted from the reactions where indicated (**F**-**I**). Scale bars: 20 μm.

Figure 8. Guanine nucleotide dependence of Rab11a-mediated membrane tethering in the presence of Myo5A-GTD and Myo5B-GTD.

(**A**) Schematic representation of liposome turbidity assays for testing Rab11a- and Myo5-GTD-dependent liposome tethering in the presence of GTP in **B**-**G**.

(**B**, **C**) Rab11a/Myo5-dependent membrane tethering is strongly and specifically promoted by the addition of GTP. Liposome turbidity assays with Rab11a-His12 (1 μM) and Myo5A-GTD (1 μM) (**B**) or Myo5B-GTD (2 μM) (**C**) were performed as in Figure 7D, E, but in the presence of GTP (1 mM).

(**D**, **E**) Liposome turbidity assays were employed with Rab11a-His12 and Myo5A-GTD (**D**) or Myo5B-GTD (**E**) as in **B**, **C**, in the presence of various concentrations of GTP (1 μM – 1 mM).

814 (**F**, **G**) Liposome turbidity assays were employed with Rab11a-His12 and Myo5A-GTD (**F**) or Myo5B-
815 GTD (**G**) as in **B**, **C**, in the presence of GTP, GTPγS, and GDP (1 mM for each).
816
817 **Figure 9.** Membrane association of Myo5-GTD proteins onto Rab11a-anchored liposomes.
818 (**A**) Schematic representation of liposome co-sedimentation assays for testing membrane binding
819 of Myo5A-GTD and Myo5B-GTD to Rab11a-bound liposomes.
820 (**B**-**G**) Liposome co-sedimentation assays were employed as in Figure 4, with Rh-labeled liposomes
821 (400 nm diameter; 1 mM lipids) and Rab11a-His12 (2 μM) (**B**, **E**), but in the presence of Myo5A-
822 GTD (2 μM) (**B-D**), Myo5B-GTD (2 μM) (**E-G**), and GTP (1 mM). For a control, the reactions without
823 Rab11a-His12 (**C**, **F**) or with the untagged form of Rab11a lacking a His12 tag (untagged Rab11a)
824 (**D**, **G**) were also tested. The supernatants (sup) and precipitates (ppt) obtained were analyzed by
825 SDS-PAGE and Coomassie Blue staining.
826
827 **Figure 10.** Myo5A-GTD and Myo5B-GTD selectively activate Rab11a-dependent membrane
828 tethering.
829 (**A**) Schematic representation of liposome turbidity assays in **B**, **C**, for the various Rab GTPases
830 (Rab11a, Rab1a, Rab4a, Rab9a, and Rab14) in the presence of Myo5-GTDs and GTP.
831 (**B**, **C**) Myo5-GTDs specifically promote efficient membrane tethering mediated by the cognate Rab
832 GTPase, Rab11a. Liposome turbidity assays were employed with Myo5A-GTD (**B**) or Myo5B-GTD
833 (**C**) and GTP, as in Figure 8B, C, but for Rab11a, Rab1a, Rab4a, Rab9a, and Rab14 GTPases.
834

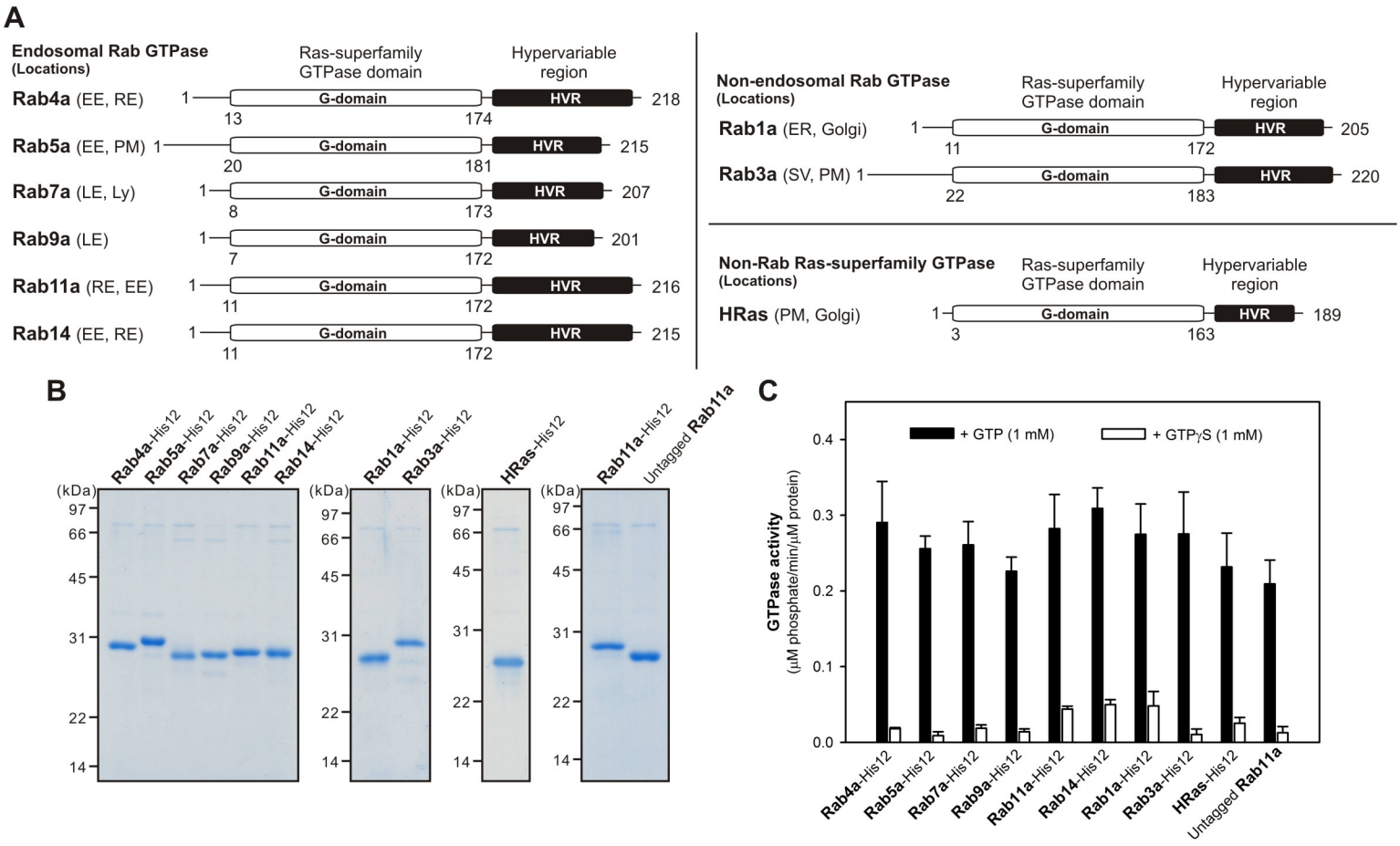

Figure 1. Purification of human Rab GTPases used in this reconstitution study.

（A) Schematic representation of theendosomal Rabs (Rab4a, Rab5a, Rab7a, Rab9a, Rab11a, and Rab14), non-endosomal Rabs (Rab1a and Rab3a), and HRas GTPase in human, showing their amino acid residues, domains (Ras-superfamily GTPase domains and hypervariable regions), andintracellular locations, which include early endosome (EE), recycling endosome (RE), plasma membrane (PM), late endosome (LE), lysosome (Ly), endoplasmic reticulum (ER), Golgi, and secretory vesicle (SV).

（B) Coomassie Blue-stained gels ofpurified recombinant proteins of the C-terminally His12-tagged endosomal Rab, non-endosomal Rab, and HRas GTPases and the untagged form of Rab11a used in this study.

（C) Intrinsic GTP-hydrolysis activities of purified Rab proteins. Purified Rab-His12, HRas-His12, and untagged Rab11a proteins (2 μM) were incubated at 30°C for 1 h in RB150 containing MgCl2 (6 mM), DTT (1 mM), and GTP (1 mM) or GTPγS (1 mM) for the control, followed by assaying released free phosphate molecules using a Malachite Green-based reagent.

Figure 1 - figure supplement 1. Inoshita & Mima

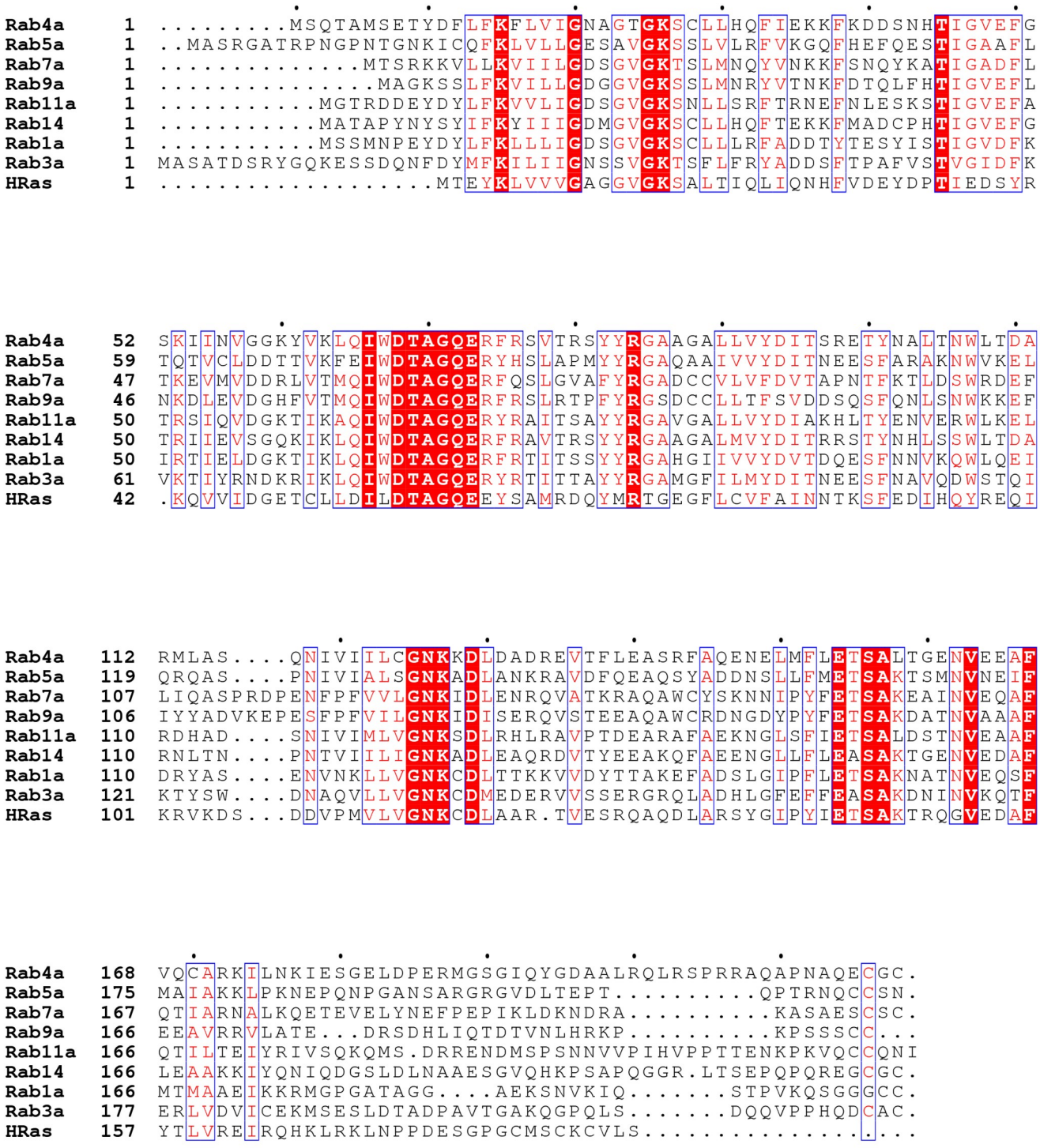

Figure 1 - figure supplement 1. Amino acid sequence alignment of the Rab- and Ras-family GTPases in human used in this study. Multiple alignment of the sequences was performed using ClustalW (http://www.genome.jp/tools/clustalw/) and ESPript 3.0 (http://espript.ibcp.fr/ESPript/ESPript/).

Figure 2. Inoshita & Mima

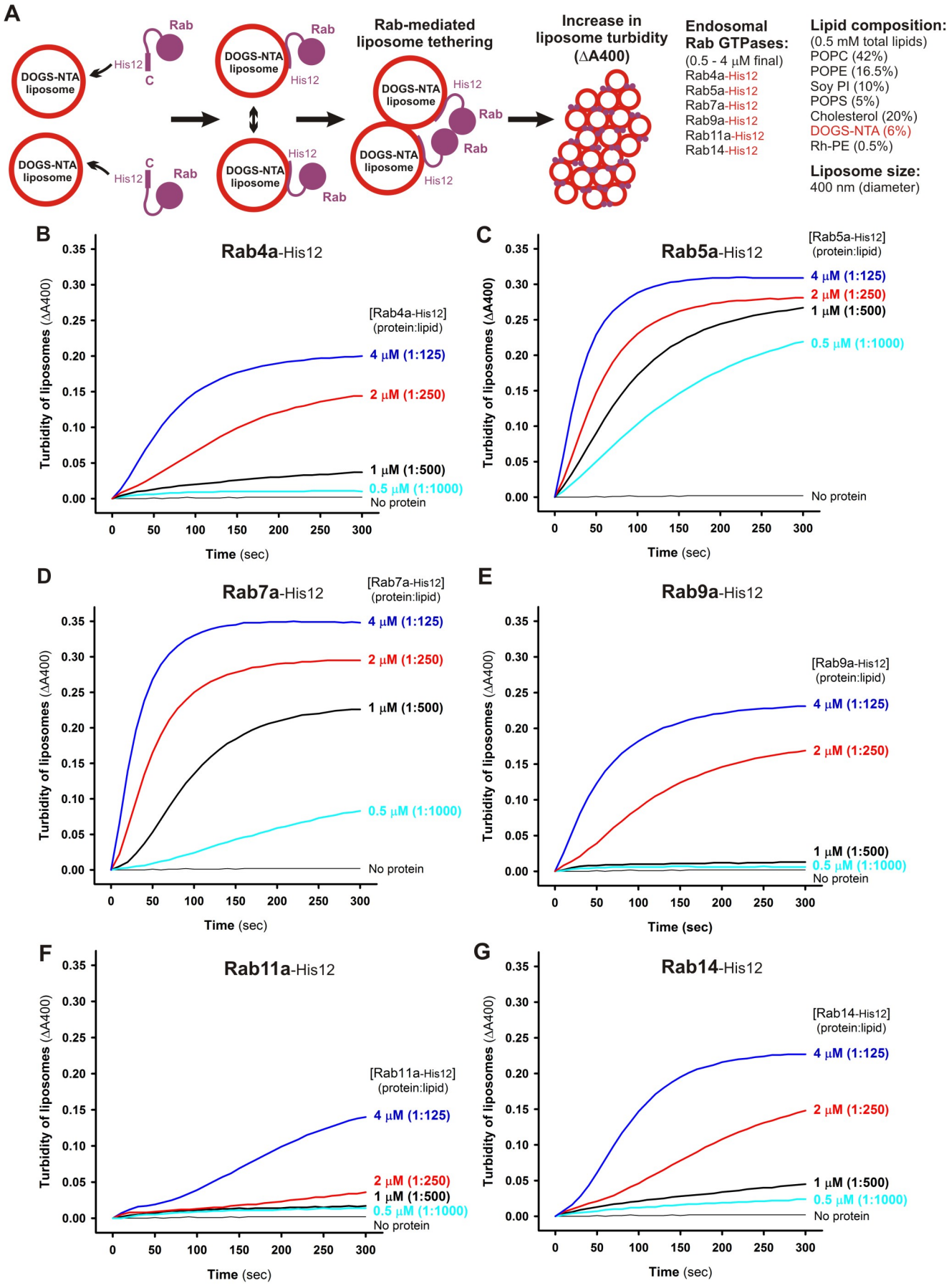

Figure 2 .Endosomal Rab GTPases directly initiate membrane tethering by themselves in a chemically defined reconstitution system.

（A) Schematic representation of liposome turbidity assays for testing Rab-mediated liposome tethering in B-G.

（B-G) Endosomal Rab-His12 proteins (0.5 - 4 μM each), Rab4a-His12 (B), Rab5a-His12 (C), Rab7a-His12 (D), Rab9a-His12 (E), Rab11a-His12 (F), and Rab14-His12 (G), were incubated with synthetic liposomes bearing physiological mimic lipid composition (400 nm diameter; 0.5 mM lipids) in RB150 containing MgCl2 (5 mM) and DTT (1 mM) at room temperature for 300 sec. During incubation, turbidity changes of the Rab-liposome mixed reactions were monitored by measuring the absorbance at 400 nm. The protein-to-lipid molar ratios used for these turbidity reactions were from 1:1000 to 1:125, as indicated.

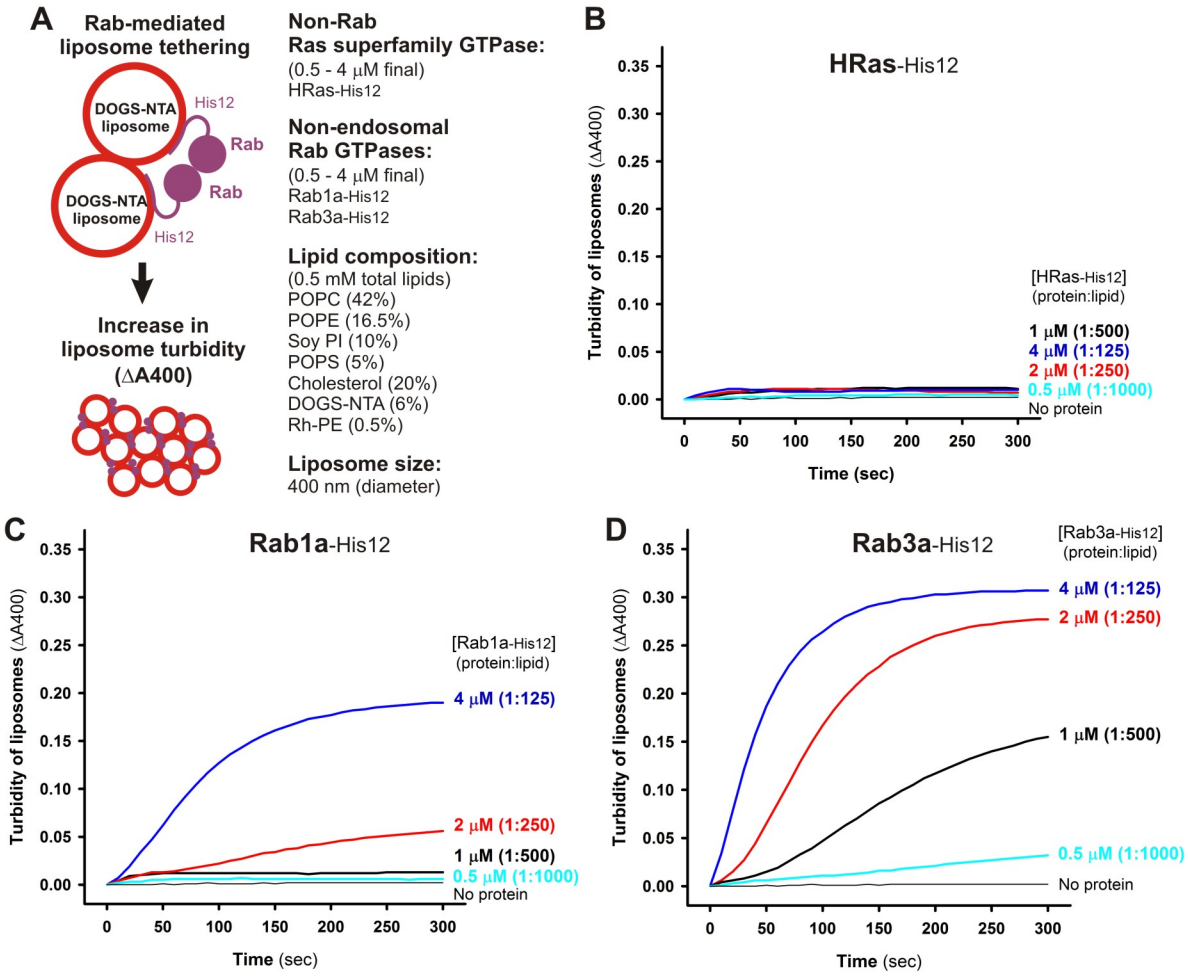

Figure 3. Non-endosomal Rab GTPases have the inherent potency to specifically mediate membrane tethering.

（A) Schematic representation of liposome turbidity assays for the non-Rab Ras superfamily GTPase, HRas, and non-endosomal Rab GTPases, Rab1a in ER-Golgi traffic and Rab3a in exocytosis, in B-D.

（B-D) Liposome turbidity assays were employed as in Figure 2B-G, with HRas-His12 (B), Rab1a-His12 (C), and Rab3a-His12 (D) proteins (0.5 - 4 μM each in final) and physiological mimic synthetic liposomes (0.5 mM total lipids in final). The protein-to-lipid molar ratios used were indicated.

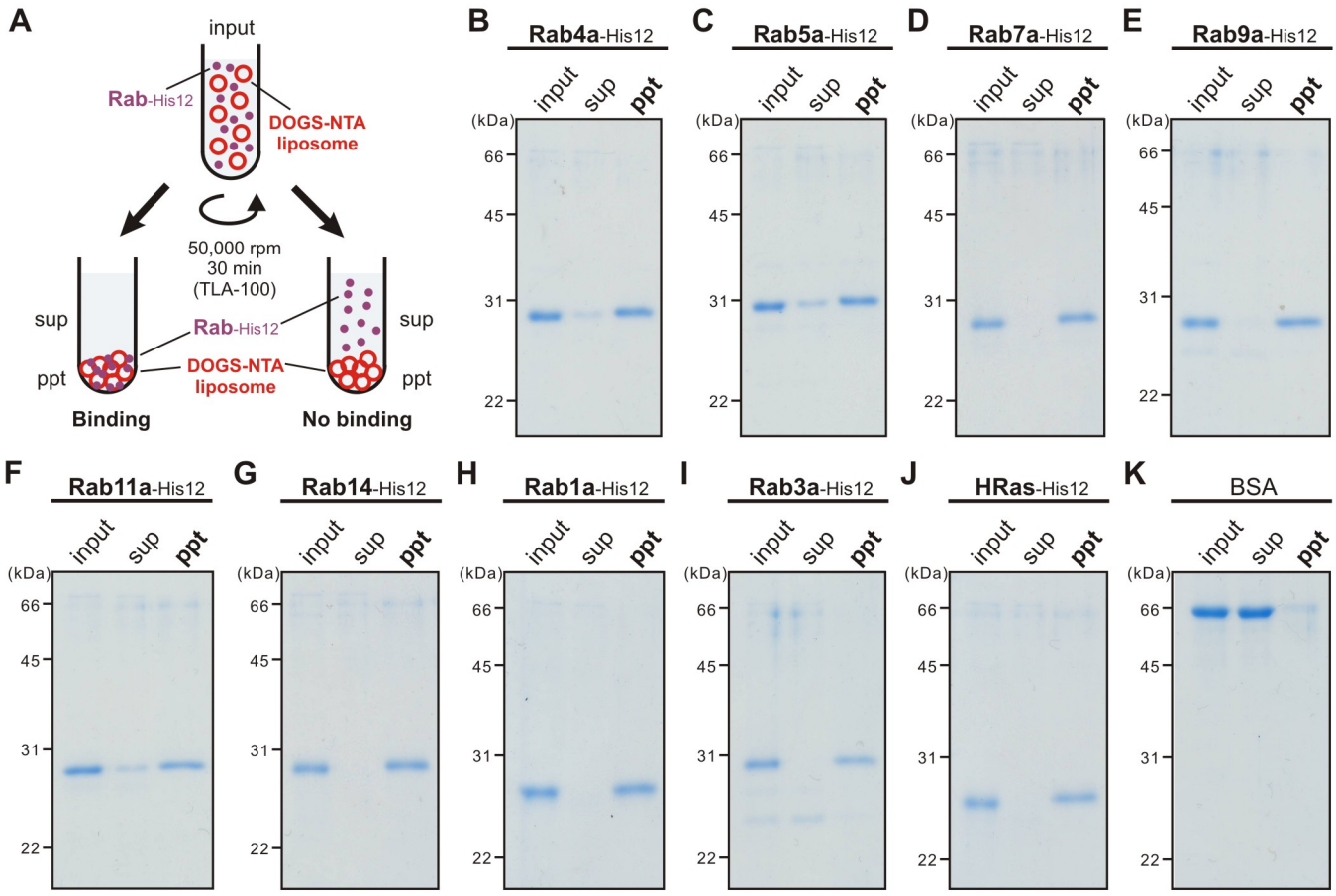

Figure 4. Membrane association of Rab-His12 proteins onto DOGS-NTA-bearing liposomes.

(A) Schematic representation of liposome co-sedimentation assays for testing membrane attachment of Rab-His12 proteins used in Figures 2-3.

(B-K) Rh-labeled liposomes (400 nm diameter; 1 mM total lipids in final) were incubated (30°C, 30 min) with Rab4a-His12 (B), Rab5a-His12 (C), Rab7a-His12 (D), Rab9a-His12(E), Rab11a-His12 (F), Rab14-His12 (G), Rab1a-His12 (H), Rab3a-His12 (I), HRas-His12 (J), and BSA for a negative control (K) (2 μM final for each), and ultracentrifuged (50,000 rpm, 30 min, 4°C). The supernatants (sup) and precipitates (ppt) obtained were analyzed by SDS-PAGE and Coomassie Blue staining.

Figure 5. Inoshita & Mima

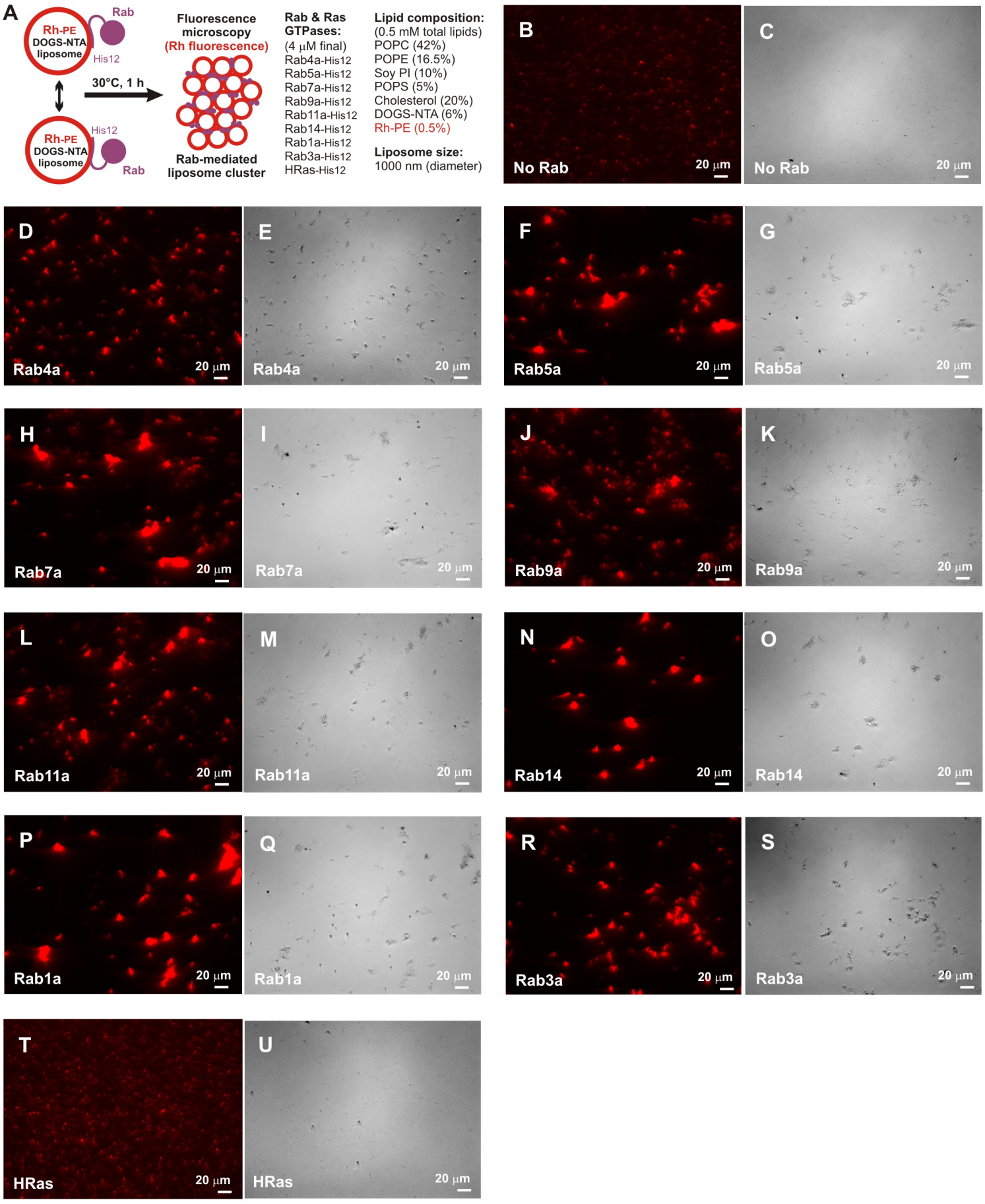

Figure 5. Rab-mediated membrane tethering induces the formation of massive liposome clusters.
（A) Schematic representation of fluorescence microscopic observations of Rab-mediated liposome clusters.
（B-U) Fluorescence images (B, D, F, H, J, L, N, P, R, T) and bright field images (C, E, G, I, K, M, O, Q, S, U) of Rab-mediated liposome clusters. Fluorescently-labeled liposomes bearing Rh-PE (1000 nm diameter; 0.5 mM lipids in final) were incubatedat 30°C for 1 h, in the absence (B, C) and presence of the Rab- and Ras-family GTPases (4 μM each in final), including Rab4a-His12 (D, E), Rab5a-His12 (F, G), Rab7a-His12 (H, I), Rab9a-His12 (J, K), Rab11a-His12 (L, M), Rab14-His12 (N, O), Rab1a-His12 (P, Q), Rab3a-His12 (R, S), and HRas-His12 (T, U),and subjected to fluorescence microscopy. Scale bars: 20 μm.

A

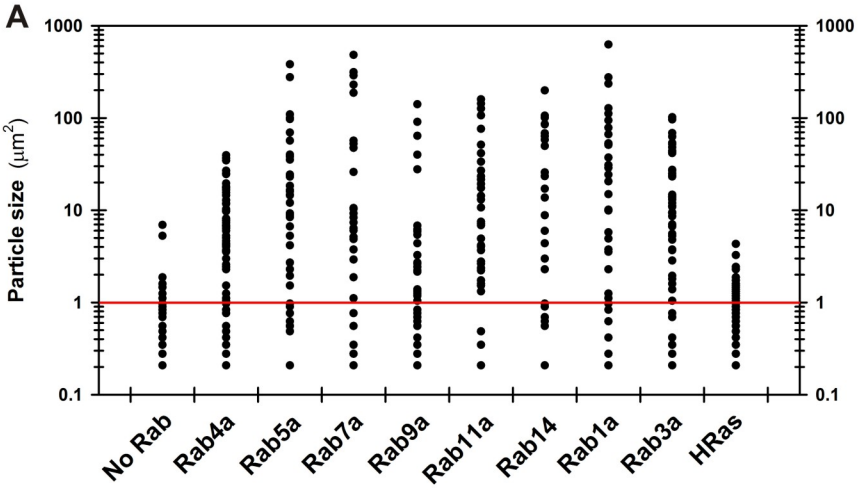

B

Rab protein	Particle number	Average size (μm²)
No Rab	38	0.92
Rab4a-His12	67	7.8
Rab5a-His12	45	32
Rab7a-His12	33	53
Rab9a-His12	55	7.9
Rab11a-His12	35	27
Rab14-His12	25	37
Rab1a-His12	36	55
Rab3a-His12	51	18
HRas-His12	96	0.80

Figure 6. Particle size distributions of liposome clusters induced by Rab-mediated membrane tethering.
（A) Particle sizes of the Rab-mediated liposome clusters observed in the fluorescence images of Figure 5.
（B) Particle numbers and average sizes of the Rab-mediated liposome clusters observed in the fluorescence images of Figure 5.

Figure 7. Inoshita & Mima

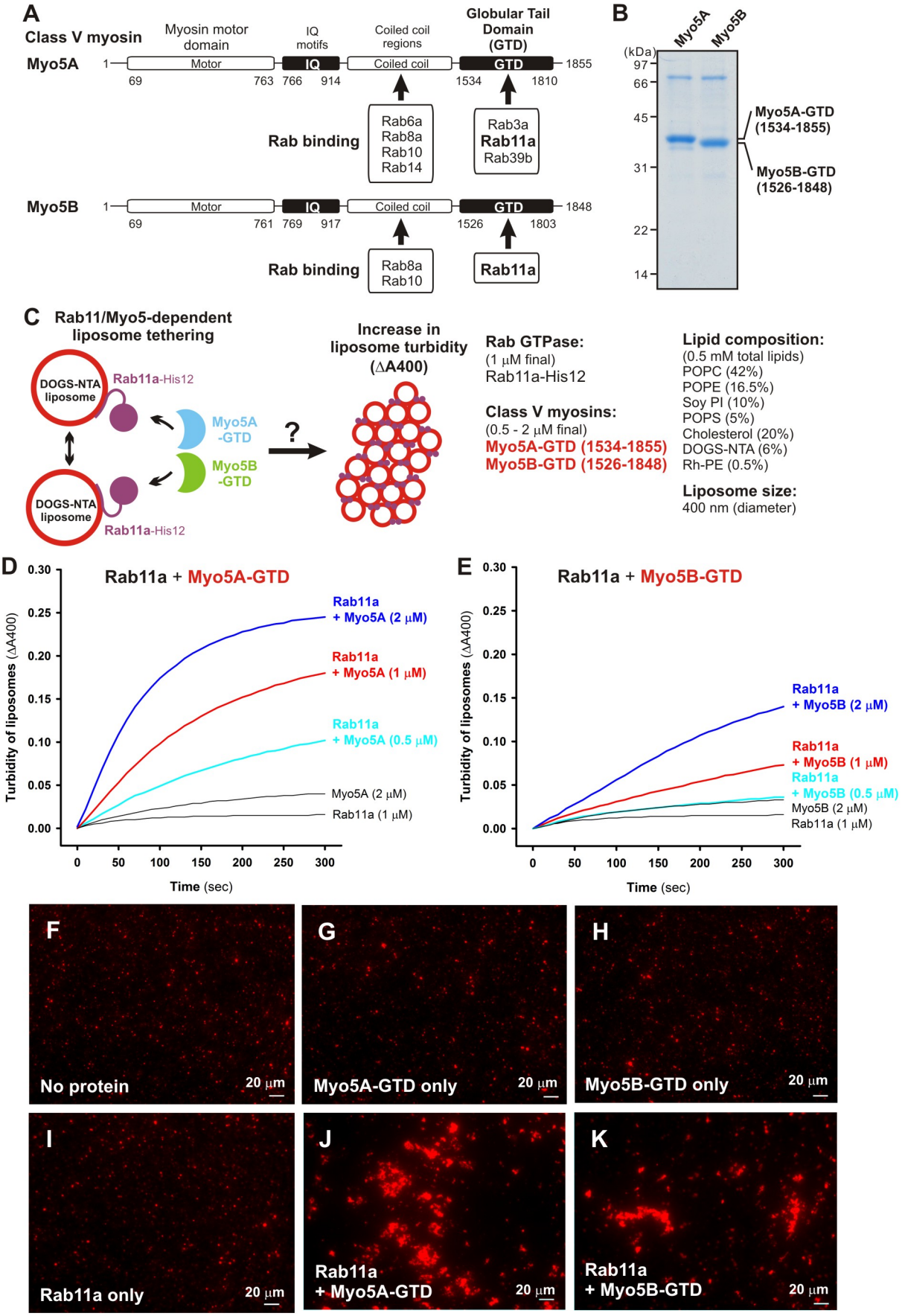

Figure 7. Class V myosin globular tail domains, Myo5A-GTD and Myo5B-GTD, strongly stimulate Rab11a-dependent membrane tethering.

（A) Schematic representation of class V myosins in human, Myo5A and Myo5B, showing their amino acid residuesand domains including myosin motor domains, IQ motifs, coiled coil regions, and globular tail domains (GTDs).Representative Myo5-interacting Rab GTPases and the Rab-binding regions in Myo5A and Myo5B are indicated.

（B) The Coomassie Blue-stained gel of purified Myo5A-GTD and Myo5B-GTD proteins, which are comprised of the amino acid residues 1534-1855 and 1526-1848, respectively.

（C) Schematic representation of liposome turbidity assays for testing Rab11a- and Myo5-GTD-dependent liposome tethering in D, E.

（D,E) Liposome turbidity assays were employed with Rab11a-His12 (1 μM final) as in Figure 2F, but in the presence of Myo5A-GTD (D) and Myo5B-GTD (E) (0.5 - 2 μM final).

（F-K) Fluorescence images of Rab11a-mediated liposome clusters in the presence of Myo5-GTDs. Rab11a-His12 (3 μM final) and Myo5A-GTD or Myo5B-GTD (3 μM final) were preincubated at 30°C for 30 min, mixed with Rh-labeled liposomes (1000 nm diameter; 0.8 mM lipids in final), further incubated (30°C, 30 min), and subjected to fluorescence microscopy (J, K). For a control, Rab11a-His12, Myo5-GTD, or both were omitted from the reactions where indicated (F-I). Scale bars: 20 μm.

Figure 8. Inoshita & Mima

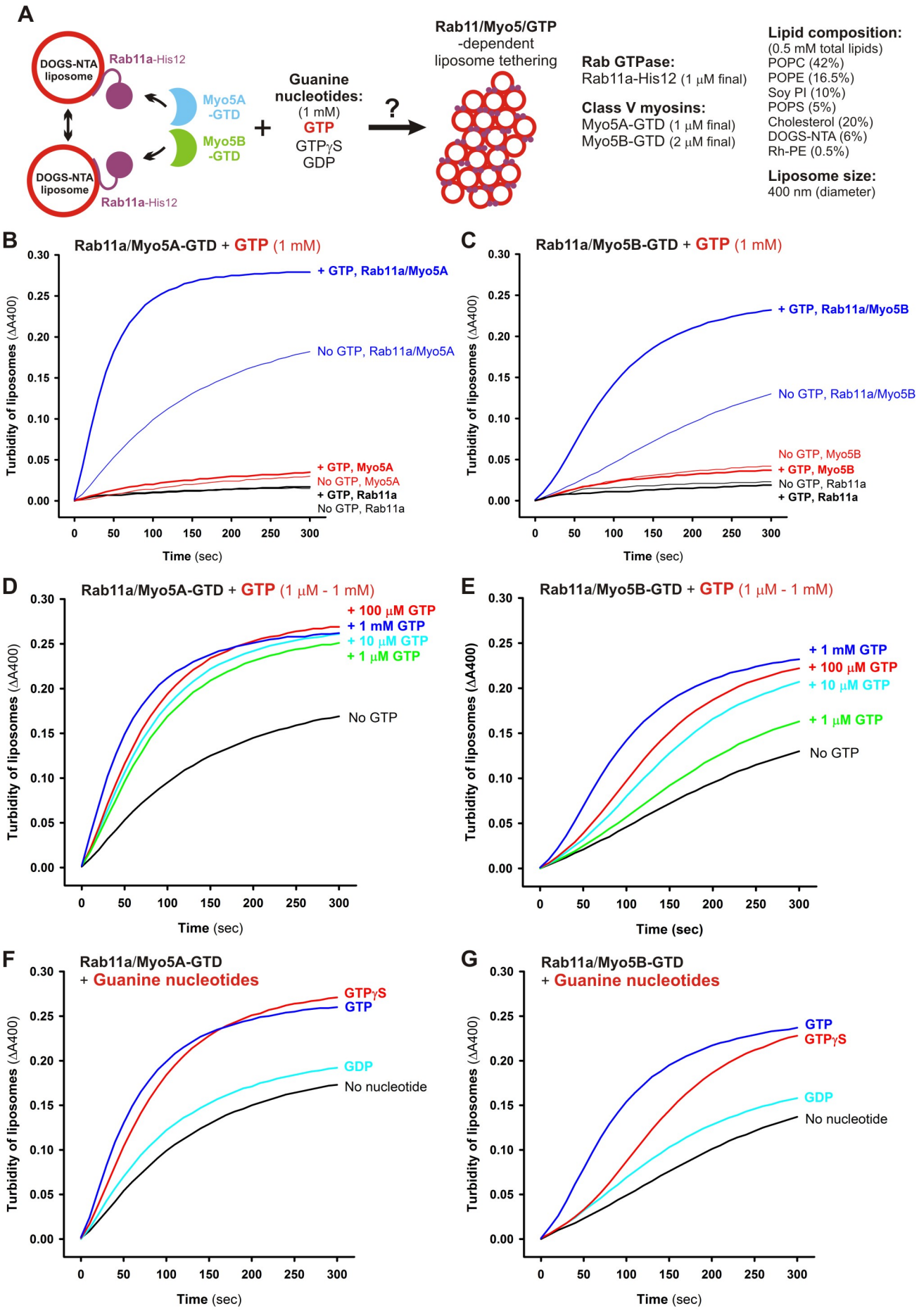

Figure 8. Guanine nucleotide dependence of Rab11a-mediated membrane tethering in the presence of Myo5A-GTD and Myo5B-GTD.

（A) Schematic representation of liposome turbidity assays for testing Rab11a- and Myo5-GTD-dependent liposome tethering in the presence of GTP in B-G.

（B, C) Rab11a/Myo5-dependent membrane tethering is strongly and specifically promoted by the addition of GTP. Liposome turbidity assays with Rab11a-His12 (1 μM) and Myo5A-GTD (1 μM) (B) or Myo5B-GTD (2 μM) (C) were performed as in Figure 7D, E, but in the presence of GTP (1 mM).

（D, E) Liposome turbidity assays were employed with Rab11a-His12 and Myo5A-GTD (D) or Myo5B-GTD (E) as in B, C, in the presence of various concentrations of GTP (1 μM - 1 mM).

（F, G) Liposome turbidity assays were employed with Rab11a-His12 and Myo5A-GTD (F) or Myo5B-GTD (G) as in B, C, in the presence of GTP, GTPγS, and GDP (1 mM for each).

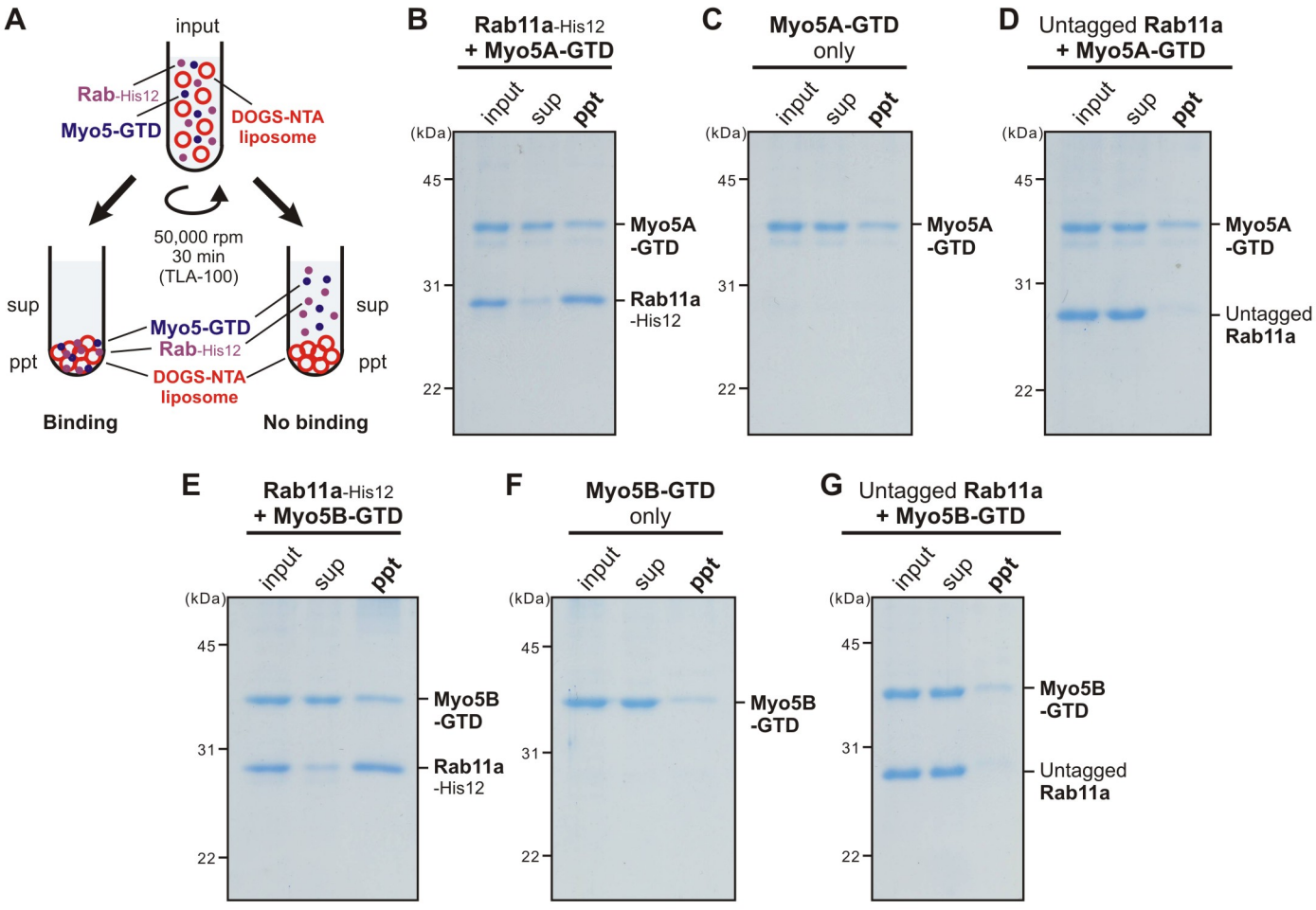

Figure 9. Membrane association of Myo5-GTD proteins onto Rab11a-anchored liposomes.

（A) Schematic representation of liposome co-sedimentation assays for testing membrane binding of Myo5A-GTD and Myo5B-GTD to Rab11a-bound liposomes.

（B-G) Liposome co-sedimentation assays were employed as in Figure 4, with Rh-labeled liposomes (400 nm diameter; 1 mM lipids) and Rab11a-His12 (2 μM) (B, E), but in the presence of Myo5A-GTD (2 μM) (B-D), Myo5B-GTD (2 μM) (E-G), and GTP (1 mM). For a control, the reactions without Rab11a-His12 (C, F) or with the untagged form of Rab11a lacking a His12 tag (untagged Rab11a) (D, G) were also tested. The supernatants (sup) and precipitates (ppt) obtained were analyzed by SDS-PAGE and Coomassie Blue staining.

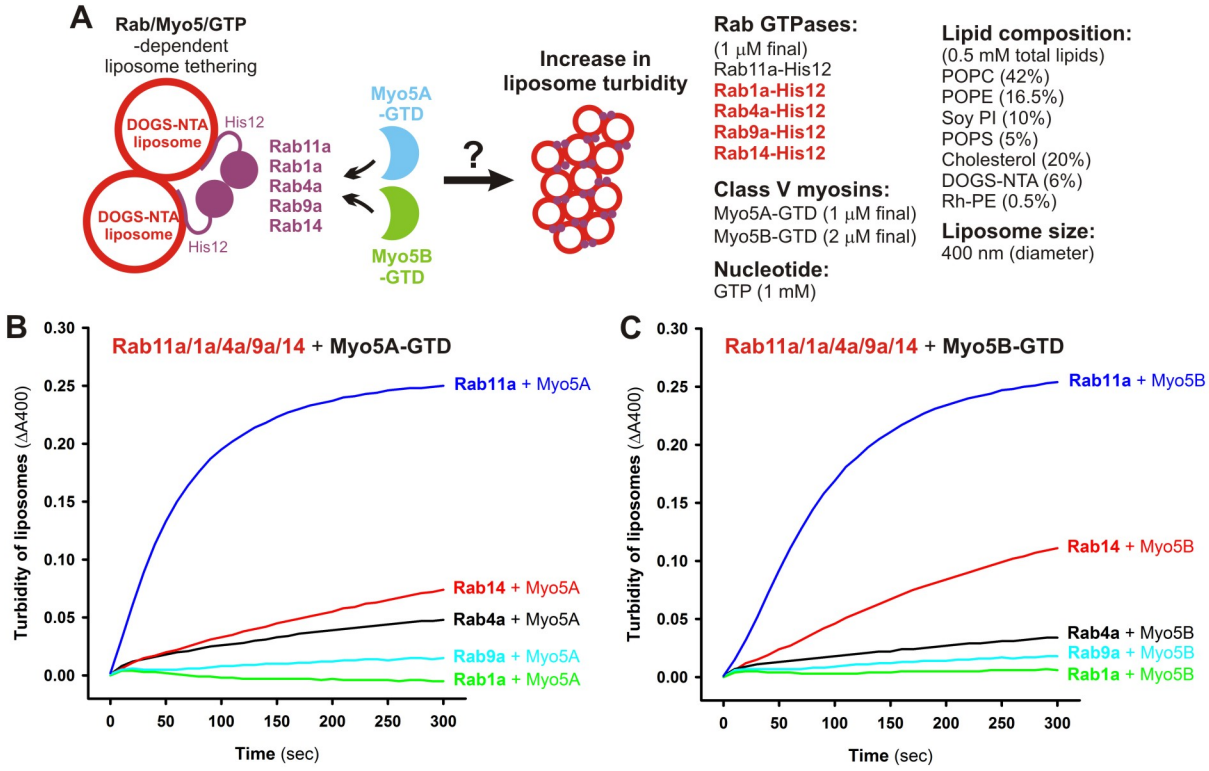

Figure 10. Myo5A-GTD and Myo5B-GTD selectively activate Rab11a-dependent membrane tethering.
(A) Schematic representation of liposome turbidity assays in B, C, for the various Rab GTPases (Rab11a, Rab1a, Rab4a, Rab9a, Rab14) in the presence of Myo5-GTDs and GTP.
(B, C) Myo5-GTDs specifically promote efficient membrane tethering mediated by the cognate Rab GTPase, Rab11a. Liposome turbidity assays were employed with Myo5A-GTD (B) or Myo5B-GTD (C) and GTP, as in Figure 8B, C, but for Rab11a, Rab1a, Rab4a, Rab9a, and Rab14 GTPases.